Newly synthesized dihydroquinazoline derivative from the aspect of combined spectroscopic and computational study

Accepted Manuscript

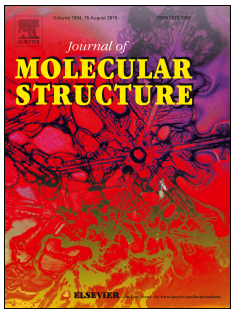

Newly synthesized dihydroquinazoline derivative from the aspect of combined spectroscopic and computational study

Adel S. El-Azab, Y. Sheena Mary, Y. Shyma Mary, C. Yohannan Panicker, Alaa A.-M. Abdel-Aziz, Magda A. El-Sherbeny, Stevan Armaković, Sanja J. Armaković, Christian Van Alsenoy

PII: S0022-2860(17)30063-7

DOI: 10.1016/j.molstruc.2017.01.044

Reference: MOLSTR 23349

To appear in: *Journal of Molecular Structure*

Received Date: 21 September 2016

Revised Date: 16 December 2016

Accepted Date: 12 January 2017

Please cite this article as: A.S. El-Azab, Y.S. Mary, Y.S. Mary, C.Y. Panicker, A.A.-M. Abdel-Aziz, M.A. El-Sherbeny, S. Armaković, S.J. Armaković, C. Van Alsenoy, Newly synthesized dihydroquinazoline derivative from the aspect of combined spectroscopic and computational study, *Journal of Molecular Structure* (2017), doi: 10.1016/j.molstruc.2017.01.044.

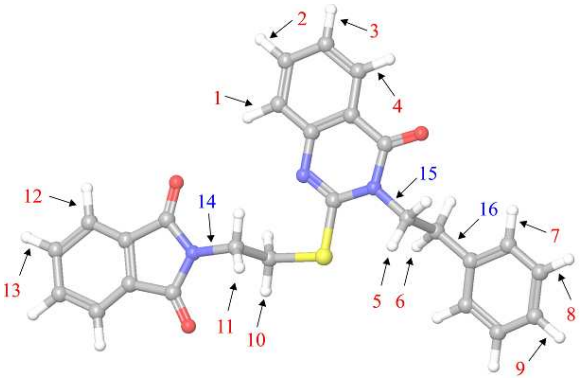

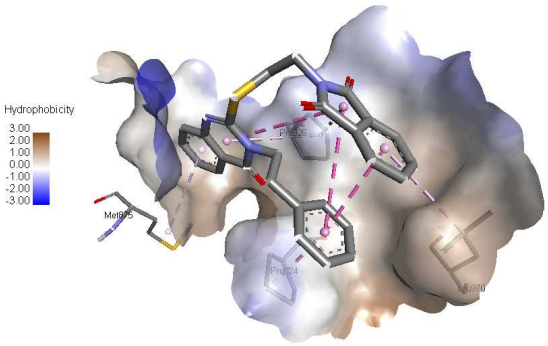

Newly synthesized dihydroquinazoline derivative from the aspect of combined spectroscopic and computational study

Adel S.El-Azab[a,b], Sheena Mary Y[c*], Shyma Mary Y[c], C.Yohannan Panicker[d], Alaa A.-M. Abdel-Aziz[a,e], Magda A. El-Sherbeny[e,f], Stevan Armaković[g], Sanja J. Armaković[h], Christian Van Alsenoy[i]

[a]Department of Pharmaceutical Chemistry, College of Pharmacy, King Saud University, Riyadh 11451, Saudi Arabia

[b]Department of Organic Chemistry, Faculty of Pharmacy, Al-Azhar University, Cairo 11884, Egypt

[c]Department of Physics, Fatima Mata National College, Kollam, Kerala, India

[d]Department of Physics, TKM College of Arts and Science, Kollam, Kerala, India

[e]Department of Medicinal Chemistry, Faculty of Pharmacy, University of Mansoura, Mansoura, Egypt

[f]Department of Pharmaceutical Chemistry, College of Pharmacy, Delta University for Science and Technology, Gamasa City, Egypt

[g]University of Novi Sad, Faculty of Sciences, Department of Physics,
Trg D. Obradovića 4, 21000 Novi Sad, Serbia

[h]University of Novi Sad, Faculty of Sciences, Department of Chemistry, Biochemistry and Environmental Protection, Trg D. Obradovića 3, 21000 Novi Sad, Serbia

[i]Department of Chemistry, University of Antwerp, Groenenborgerlaan 171, B-2020 Antwerp, Belgium

*author for correspondence: email: sypanicker@rediffmail.com

Abstract

In this work, spectroscopic characterization of 2-(2-(4-oxo-3-phenethyl-3,4-dihydroquinazolin-2-ylthio)ethyl)isoindoline-1,3-dione have been obtained with experimentally and theoretically. Complete assignments of fundamental vibrations were performed on the basis of the potential energy distribution of the vibrational modes and good agreement between the experimental and scaled wavenumbers has been achieved. Frontier molecular orbitals have been used as indicators of stability and reactivity. Intramolecular interactions have been investigated by NBO analysis.

The dipole moment, linear polarizability and first and second order hyperpolarizability values were also computed. In order to determine molecule sites prone to electrophilic attacks DFT calculations of average local ionization energy (ALIE) and Fukui functions have been performed as well. Intra-molecular non-covalent interactions have been determined and analyzed by the analysis of charge density. Stability of title molecule have also been investigated from the aspect of autoxidation, by calculations of bond dissociation energies (BDE), and hydrolysis, by calculations of radial distribution functions after molecular dynamics (MD) simulations. In order to assess the biological potential of the title compound a molecular docking study towards breast cancer type 2 complex has been performed.

Keywords: DFT; ALIE; RDF; BDE; Quinazoline; molecular docking.

1. Introduction

Dihydroquinazoline derivatives are important classes of heterocyclic compounds and possess a broad spectrum of biological and pharmaceutical activities such as analgesic, antitumor, anticancer, diuretic and herbicide activities [1]. These compounds can be easily be oxidized to their quinazolin analogues [2, 3], which also include important pharmacologically active compounds [4-14]. Jiaang et al. [15] reported the synthesis of novel isoindoline compounds for potent and selective inhibition of prolyl dipeptidase DPP8. The heterocyclic spirooxindole ring system is widely distributed structural framework that is present in a number of pharmaceuticals and natural products [16] including cytostatic alkaloids like spirotryprostatins and strychnophylline [17]. Spriooxindole compounds are attractive synthetic targets because of the unique structural array property and the highly pronounced pharmacological activity displayed by them [18, 19]. Alanazi et al. [9, 20] reported the synthesis, biological, antitumor and antimicrobial activities of certain quanzoline derivatives. All of the aforementioned studies motivated us to synthetize new dihydroquinazoline derivative and to thoroughly investigate it from the aspects of spectroscopic characterization and reactivity study by DFT and MD methods. The density functional theory is a well known method for the calculation of molecular structures, vibrational wavenumbers and energies of molecules. HOMO and LUMO analyses were used to determine the charge transfer within the molecule and such molecular properties as ionization potential, electron affinity, electronegativity, chemical potential and global electrophilicity index. Due to the different potential biological activity of the title compound, molecular docking study is also reported. Due to interesting properties newly synthetized dihydroquinazoline derivative

presented in this study could serve as an active component of some drug. When it comes to the ecological aspects, degradation of pharmaceutical molecules is separate issue. Due to their high stability these molecules accumulate in water resources and they are often toxic to aquatic organisms [21, 22]. In the same time conventional methods for water purification are no longer efficient and economic [23, 24]. Alternative approaches for the removal of these substances from water include the so called forced degradation which is based on advanced oxidation processes [22, 23, 25, 26]. Therefore, in order to understand degradation properties of the title compound we have performed DFT calculations of bond dissociation energy (BDE) and calculations of radial distribution functions after MD simulations. Studies of degradation properties are time consuming and therefore DFT calculations and MD simulations are frequently employed in order to significantly rationalize experimental procedures [27-30]. BDE is related to the hydrogen abstraction and reflects the sensitivity of molecule towards autoxidation mechanism. On the other side RDFs indicate which atoms of the title molecule have pronounced interactions with water molecules, providing information on the possible influence of hydrolysis mechanisms.

2. Experimental details

A mixture of 2-mercapto-3-phenethylquinazolin-4(3*H*)-one (2 mmol, 564 mg) and 2-(2-chloroethyl)isoindoline-1,3-dione (2.1 mmol, 440 mg) in 15 ml acetone containing anhydrous potassium carbonate (3 mmol, 415 mg) was stirred at room temperature for 12 h. The reaction mixture was filtered, the solvent was removed under reduced pressure and the solid obtained was dried and re-crystallized from ethanol. Mp: 202–204 ^{o}C, yield 84 %, MS: (MS = 455, 63, 100 %). Nuclear magnetic resonance (^{1}H and ^{13}C NMR) spectra were recorded on Bruker 500 MHz spectrometer using $CDCl_3$ as solvent; the chemical shifts are expressed in δ ppm using TMS as internal standard. The FT-IR spectrum (Fig.1) was recorded using KBr pellets on a DR/Jasco FT-IR 6300 spectrometer. The FT-Raman spectrum (Fig.2) was obtained on a Bruker RFS 100/s, Germany. For excitation of the spectrum the emission of Nd:YAG laser was used, excitation wavelength was 1064 nm, maximal power was 150 mW and measurement was carried out on solid sample.

3. Computational details

Calculations (wavenumbers, molecular electrostatic potential, frontier molecular orbital analysis, natural bond orbital analysis, nonlinear optical properties, and NMR) of the title compound were carried out using Gaussian09 software [31] with the B3LYP/6-

311++G(d,p)(5D,7F) basis set [32, 33]. The theoretically obtained wavenumbers are scaled by using the scaling factor 0.9613 [34] and the optimized geometrical parameters (Fig.3) of the title compound are given in Table S1 (supporting information). The assignments of the calculated wave numbers are aided by using GAUSSVIEW [35] and GAR2PED software [36].

Beside Gaussian software package further insights into the reactive properties of title molecule have been obtained by application of Schrödinger Materials Science Suite 2015-4. Concretely, Jaguar 9.0 program [37] has been applied for DFT calculations, while Desmond program has been applied for MD simulations [38-41]. DFT calculations performed with Jaguar have been done with B3LYP exchange-correlation functional [42]. For calculations of ALIE, Fukui functions and BDEs, 6-311++G(d,p), 6-31+G(d,p) and 6-311G(d,p) basis sets have been used, respectively. In the case of MD simulations OPLS 2005 force field [43] was used. Simulation time of 10 ns andisothermal–isobaric (NPT) ensemble class were also used. To model the interactions of title molecule with water one title molecule has been placed in the cubic box with ~3000 water molecules at temperature of 300 K and pressure of 1.0325 bar. Cut off radius was set to 12 Å, while solvent was modeled by simple point charge (SPC) model [44]. Determination of noncovalent interactions in Jaguar program is based on the methods developed by Johnson [45, 46].

4. Results and discussion

In the following discussion, the C_{25}-C_{26}-C_{28}-C_{30}-C_{32}-C_{34} (mono), C_8-C_9-C_{11}-C_{13}-C_{15}-C_{17} (ortho) and C_{44}-C_{45}-C_{47}-C_{49}-C_{51}-C_{53} (ortho) phenyl rings are designated as PhI, PhII and PhIII respectively. The quinazoline and isoindoline rings are designated as PhV and PhIV.

4.1. Geometrical parameters

The bond lengths of C_{43}-N_2 (1.4069 Å), C_{54}-N_2 (1.4042 Å), C_{40}-N_2 (1.4596 Å), C_8-N_6 (1.3824 Å), C_{18}-N_7 (1.4181 Å), C_{19}-N_7 (1.4754 Å) and C_{36}-N_7 (1.3835 Å) are shorter than the normal C-N bond length (1.48 Å) [47]. In the title compound, the C-S bond lengths are 1.7928 and 1.8296 Å while the reported values are in the range 1.7675-1.8641 Å [48] and 1.7710-1.8110 Å [49]. The shortening of the carbonyl bond lengths (C_{43}-O_4 = 1.2083 Å, C_{54}-O_5 = 1.2098 Å, C_{18}-O_3 = 1.2206 Å) shows double bond character. The C-C bond lengths in the phenyl rings of the title compound lie in the range 1.3932-1.4001 Å for PhI, 1.3834-1.4088 Å for PhII and 1.3939-1.3991 Å for PhIII [50]. The quinazoline moiety, PhV is planar with respect to the phenyl ring PhII, as is evident from the torsion angles C_{15}-C_{17}-C_{18}-N_7 = 179.0˚, C_{15}-C_{17}-C_8-N_6 =

1798.8˚, C_9-C_8-N_6-C_{36} = -178.9˚ and C_9-C_8-C_{17}-C_{18} = 179.4˚. The CH_2 groups at C_{19} and C_{22} are tilted from the phenyl ring PhI and the quninazoline ring PhV, as is evident from the torsion angles, C_{28}-C_{26}-C_{25}-C_{22} = 178.5˚, C_{26}-C_{25}-C_{22}-C_{19} = -83.0˚, C_{32}-C_{34}-C_{25}-C_{22} = -178.5˚, C_{34}-C_{25}-C_{22}-C_{19} = 95.4˚ and C_{17}-C_{18}-N_7-C_{19} = -179.9˚, C_{18}-N_7-C_{19}-C_{22} = -85.3˚, N_6-C_{36}-N_7-C_{19} = -179.6˚, C_{36}-N_7-C_{19}-C_{22} = 93.1˚. The isoindoline fragment is also planar with respect to the phenyl ring PhIII, as is evident from the torsion angles, C_{45}-C_{44}-C_{43}-N_2 = -180.0˚, C_{45}-C_{44}-C_{53}-C_{54} = -179.9˚, C_{51}-C_{53}-C_{54}-N_2 = 180.0˚ and C_{51}-C_{53}-C_{44}-C_{43} = 179.9˚. At C_{43} and C_{54} positions the exocyclic angles, N_2-C_{43}-O_4 = 125.5˚, O_4-C_{43}-C_{44} = 128.9˚ and N_2-C_{54}-O_5 = 125.0˚, O_5-C_{54}-C_{53} = 129.2˚, respectively and this asymmetry of angles reveal the interaction between isoindoline-1,3-dione and adjacent moieties. Similarly at N_2 position, the bond angles, C_{43}-N_2-C_{40} and C_{54}-N_2-C_{40} are increased by 4.5˚ and 3.4˚ from 120˚ which show the interaction between the carbonyl groups with the adjacent CH_2 groups. Also at C_{36} position, the bond angle N_7-C_{36}-N_6 = 125.0˚ and this enlargement from 120˚ shows the interaction between the adjacent groups and quinazoline moiety. At C_{18} position bond angle C_{17}-C_{18}-N_7 = 114.7˚ and C_{17}-C_{18}-O_3 = 125.2˚, and this variation gives the interaction between O_3 and CH_2 group at C_{19} position. This is supported by the bond angle values, C_{18}-N_7-C_{19} = 116.3˚ and C_{36}-N_7-C_{19} = 122.9˚ at N_7 position.

4.2. IR and Raman spectra

IR and Raman spectroscopy are standard characterization techniques that allow clear identification of molecules and provide an insight into some specific physico-chemical properties. Regarding IR and Raman spectroscopy it is also important to note that DFT calculations can be readily applied for the prediction of these spectra and therefore allow prediction of some specific molecular properties. Theoretical IR and Raman calculations also serve as confirmation of the used level of theory. Namely, if calculated and measured spectra agrees well than the employed level of theory can be considered as good choice for obtaining reliable results. The calculated (scaled) wavenumbers, observed IR, Raman bands and assignments are provided in table 1.

The bands observed at 1760, 1708, 1668 cm^{-1} in the IR spectrum, 1761, 1715, 1667 cm^{-1} in the Raman spectrum and at 1752, 1700, 1663 cm^{-1} (DFT) are assigned as the stretching modes of C=O, which are expected in the range 1850-1550 cm^{-1} [51]. All the three C=O stretching modes are IR and Raman active with PEDs greater than 73%. The in-plane and out-of-plane bending modes of C=O are expected in the ranges 725 ± 95 and 595 ± 120 cm^{-1} [52] and in the

present case, C=O deformation bands are assigned at 841, 776, 766, 697, 672 and 617 cm^{-1} theoretically (DFT) with PEDs 41 to 76%.

In the title compound, the band observed at 631 cm^{-1} in the IR spectrum and 729, 633 cm^{-1} (DFT) are assigned as the C-S stretching modes. The C-N stretching modes are assigned at 1152, 1111 cm^{-1} (IR), 1323, 1206, 1106 cm^{-1} (Raman) and in the range 1322-955 cm^{-1} theoretically which are in agreement with literature and having PED 40 to 50% [52-54]. The C-N stretching modes are reported at 1283 cm^{-1} in the IR spectrum, 1286, 1243 cm^{-1} in the Raman spectrum and at 1283, 1240, 1119 cm^{-1} theoretically for a quinazoline derivative [55]. For the title compound, the C=N stretching mode is assigned at 1526 cm^{-1} theoretically as expected with a PED of 40% [52].

The stretching and deformation modes of CH_2 group appear in the regions 3020-2875, 1480-725 cm^{-1} respectively [52-54]. The CH_2 stretching modes are observed at 3027, 2976, 2955 cm^{-1} (IR), 2998, 2956, 2925 cm^{-1} (Raman) and in the range 3029-2928 cm^{-1} theoretically. The deformation modes of CH_2 are assigned at 1391, 1355, 1332, 1275, 1238, 715 cm^{-1} (IR), 1393, 1349, 1335, 1274, 1236, 712 cm^{-1} (Raman) and in the ranges 1441-1389 (scissoring), 1356-1308 (wagging), 1271-1226 (twisting), 1071-713 (rocking) cm^{-1} theoretically as expected [52-54].

For phenyl rings, the C-H stretching modes are expected above 3000 cm^{-1} [52] and for the title compound, the CH stretching modes are assigned in the range 3065-3032 cm^{-1} for PhI, 3078-3045 cm^{-1} for PhII and 3077-3051 cm^{-1} for PhIII rings theoretically. Experimentally bands are observed at 3082, 3055 cm^{-1} in IR and 3080, 3060, 3043 cm^{-1} in Raman spectrum. The phenyl ring stretching modes are assigned at 1578, 1469, 1428 cm^{-1} (IR), 1582, 1467 cm^{-1} (Raman), in the range 1580-1290 cm^{-1} (DFT) for PhI, 1547, 1446 cm^{-1} (IR), 1582, 1551, 1307 cm^{-1} (Raman), in the range 1582-1306 cm^{-1} (DFT) for PhII and 1332, 1166 cm^{-1} (IR), 1582, 1438, 1335, 1160 cm^{-1} (Raman), in the range 1582-1163 cm^{-1} (DFT) for PhIII.

The wavenumber intervals for the ring breathing mode of ortho substituted phenyl rings are: 1100-1130 cm^{-1} for heavy substituent, 1020-1070 cm^{-1}, when one of the substituent is light and 630-780 cm^{-1} for light substituent [56]. In the present case the PED analysis gives ring breathing modes at 978 cm^{-1} for PhI, 1084 cm^{-1} for PhII and 1055 cm^{-1} for PhIII, as expected [52]. For ortho substituted phenyl ring, the ring breathing mode is reported at 1041 cm^{-1} [57] and at 1086, 1011 cm^{-1} (theoretically) [58] and at 1020 cm^{-1} (theoretically) [59]. The ring breathing modes of phenyl rings PhI and PhII are 63% while the ring breathing mode of PhIII is only 45%

and this mode is mixed with a contribution of 48% PED due to in-plane CH bending mode of the phenyl ring.

The C-H deformation modes of the phenyl ring, in-plane and out-of-plane modes are expected above and below 1000 cm^{-1} respectively [52]. For the title compound, the in-plane CH deformation modes are assigned at 1012 cm^{-1} (Raman) for PhI, 1152, 1005 cm^{-1} (IR), 1002 cm^{-1} (Raman) for PhII and 1048 (IR), 1135, 1050 cm^{-1} (Raman) for PhIII. The DFT calculations give these modes in the ranges 1310-1009 cm^{-1} for PhI, 1256-1007 cm^{-1} for PhII and 1259-1055 cm^{-1} for PhIII, as expected [52]. The out-of-plane C-H modes are assigned at 963, 893 cm^{-1} (IR), 963, 962, 947, 891, 825 cm^{-1} (DFT) for PhI, 969, 754 cm^{-1} (Raman), 967, 951, 861, 753 cm^{-1} (DFT) for PhII and 973, 945, 872, 773 cm^{-1} (DFT) for PhIII.

4.3. Molecular Electrostatic Potential (MEP)

Molecular electrostatic potential serves as a relatively inexpensive quantum-molecular descriptor which indicates charge distribution within molecule of interest. Best visualization in the case of this descriptor is obtained by mapping of MEP values to the electron density surface and such surface is called MEP surface. Obtained results in the case of MEP surface indicate critical molecule sites, from the aspect of maximal and minimal MEP values, and therefore determine molecule sites prone to specific types of attack. The MEP surface in the case of title molecule is provided in Fig. 4. The electrostatic potential values at the surface are represented as follows; red color, regions of most electro negative electrostatic potential, blue color, regions of most positive electrostatic potential and green color, regions of zero potential. The electrostatic potential increases in the order red < orange < yellow < green < blue [60]. As can be seen from the Fig. 4, the negative electrostatic potential regions are mainly localized over the oxygens of the carbonyl groups and the phenyl rings PhI and PhII and are possible sites for electrophilic attack. The positive regions are localized over the nitrogen atoms as possible sites for nucleophilic attack.

4.4 ALIE surface, Fukui functions and indices, and non-covalent interactions

It was shown by Sjoberg et al. [61] that ALIE values can be valuable indicators of reactivity of aromatic compounds [62]. This quantum molecular descriptor is sum of orbital energies weighted by the orbital densities:

$$I(r) = \sum_i \frac{\rho_i(\vec{r})|\varepsilon_i|}{\rho(\vec{r})}, \quad (1)$$

and it indicates the molecule locations where electrons are least tightly bound, i.e. the molecule sites for which the possibility to be prone to electrophilic attacks is the highest. In the equation (1) $\rho_i(\vec{r})$ stands for the electronic density of the *i*-th molecular orbital at the point $\vec{r}$, ε_i stands for the orbital energy, while $\rho(\vec{r})$ stands for the total electronic density function. Probably the best way to practically use the information on ALIE values is to map them to the electron density surface, which has been done in Fig. S1 (supporting information).

According to the results presented in Fig. S1, there are two specific locations where red color, which designates the lowest ALIE values, is located. Namely, red color is located in the near vicinity of sulfur S1 atom and, to somewhat smaller extent, in the near vicinity of terminal benzene ring. In these cases ALIE has values around 190 kcal/mol. On the other side the highest ALIE values and locations where electrons are the most tightly bound can be seen in the near vicinity of nitrogen atoms and hydrogen atoms of aforementioned benzene ring, with the values of around 343 kcal/mol.

Analysis of charge density between non-bonded atoms, according to the method by Johnson et al. [45, 46] yielded three distinct intra-molecular non-covalent interactions. These interactions are located between atoms O4–H10, N6–H42 and S1–H39, with the strongest being located between S1– H39 characterized by the strength value of –0.016 electron/bohr^3. Intra-molecular non-covalent interactions have been visualized in Fig. S2 (supporting information).

The concept of Fukui functions is based on the analysis of electron density changes upon addition or removal of charge. This tool allows further insight into the local reactivity properties of investigated molecule. Two Fukui functions, f^+ and f^-, in Jaguar program can be calculated in the finite difference approximation [63].

In this work for the purpose of visualization of molecule areas where charge density has been increased or decreased, values of f^+ and f^- functions have been mapped to the electron density surface, Fig. S3 (supporting information). Increase in electron density after addition of charge in the case of Fukui f^+ function in Fig. S3a has been marked by positive (purple and blue-to-purple) colors, while decrease in electron density after removal of charge in the case of Fukui f^- function has been marked by the negative (red) color. Results presented in Fig. S3a indicate that after charge addition electron density increases in the area of molecule where six- and five-membered rings are fuzzed, including oxygen atoms O4 and O5, therefore indicating that these parts of the molecule act as an electrophile after the addition of charge. On the other side red

color in Fig. S3b show that near vicinities of the oxygen atom O4 and hydrogen atoms H42 and H38 are deficient in terms of electron density, therefore indicating that this part of molecule acts as a nucleophile after the removal of charge.

Beside Fukui functions is also useful to calculate Fukui indices which also indicate the propensity of the electron density to deform at a given position upon accepting or donating electrons [64, 65]. Fukui indices are also called condensed or atomic Fukui functions on the j^{th} atom site are defined as:

$$f_j^- = q_j(N) - q_j(N-1) \qquad (2)$$

$$f_j^+ = q_j(N+1) - q_j(N) \qquad (3)$$

$$f_j^0 = \frac{1}{2}[q_j(N+1) - q_j(N-1)] \qquad (4)$$

For an electrophilic, $f_j^-(r)$, nucleophilic or free radical attack $f_j^+(r)$, on the reference molecule, respectively. In these equations, q_j is the atomic charge (evaluated from Mulliken population analysis, electrostatic derived charge, etc.) at the j^{th} atomic site is the neutral (N), anionic (N + 1) or cationic (N -1) chemical species. Chattarajet al. [66] proposed the concept of generalized philicity which gives almost all information about the known different global and local reactivity and selectivity descriptor, in addition to the information regarding electrophilic/nucleophilic power of a given atomic site in a molecule. Morell et al. [67] have proposed a dual descriptor (Δf(r)), which is defined as the difference between the nucleophilic and electrophilic Fukui function and is given by,

$$\Delta f(r) = [f^+(r) - f^-(r)] \qquad (5)$$

$\Delta f(r) > 0$, then the site is favored for a nucleophilic attack, whereas if $\Delta f(r) < 0$, then the site may be favored for an electrophilic attack and the reactivity descriptor Δf(r) provides useful information on both stabilizing and destabilizing interactions between a nucleophile and an electrophile and helps in identifying the electrophilic/nucleophilic behaviour of a specific site within a molecule. It provides positive value which is mostly in S1, N6 (positive value i.e. Δf(r) > 0) for site prone for nucleophilic attack and a negative value lies in O4, O5, C43, H46 (negative value i.e. Δf(r) < 0) prone for electrophilic attack and these values reported in Table S2 (supporting information).

4.5 Frontier Molecular Orbital analysis

Frontier molecular orbitals are mainly responsible for the reactivity in the case of organic molecules such as the title one investigated in the present work. The distribution of the highest occupied molecular orbital (HOMO) indicates molecule site available to donate electrons, while the distribution of the lowest unoccupied molecular orbital (LUMO) determine molecule sites able to receive electrons. In the same time information on energies of the frontier molecular orbitals can be used for the calculation of several important quantities that reflect global stability and reactivity properties of molecule. The pictorial representation of the HOMO and the LUMO is shown in Fig.5. The HOMO lies at -7.386 eV and whereas the LUMO is located at -5.584 eV and HOMO is delocalized over the phenyl ring PhII, quinazoline ring PhV, sulfur atom, CH_2 groups at C_{37}, C_{40} and the nitrogen atom N_2 of isoindoline ring while the LUMO is located at phenyl ring PhIII and isoindoline ring with the exception of the nitrogen atom N_2. This shows that an eventual charge transfer occurs within the molecule, and that the frontier orbital energy gap is 1.802 eV. By using the HOMO and LUMO energy values, the global chemical reactivity descriptors such as hardness, chemical potential, electro-negativity and electrophilicity index as well as local reactivity can be defined [68]. Pauling introduced the concept of electro-negativity as the power of an atom in a molecule to attract electrons to it. Hardness (η), chemical potential (μ) and electro-negativity (χ) are defined using Koopman's theorem as $\eta = (I-A)/2 = 0.901$ eV, $\mu = -(I+A)/2 = -6.485$ eV and $\chi = (I+A)/2 = 6.485$ eV, where A and I are the ionization potential and electron affinity of the molecule. $I = -E_{HOMO} = 7.386$ eV and $A = -E_{LUMO} = 5.584$ eV. Parr *et al*. [69] have defined a descriptor to quantify the global electrophilic power of the molecule as the electrophilicity index, $\omega = \mu^2/2\eta = 23.338$ eV.

4.6 Natural Bond Orbital analysis (NBO)

The natural bond orbitals (NBO) calculations were performed using NBO 3.1 program [70] as implemented in the Gaussian09 package at the DFT/B3LYP level and the results are given in Tables 2 and 3. The various important intra-molecular hyper-conjugative interactions are: N_6-C_{36} from S_1 of $n_1(S_1)\rightarrow\pi^*(N_6\text{-}C_{36})$, O_5-C_{54} from N_2 of $n_1(N_2)\rightarrow\pi^*(O_5\text{-}C_{54})$, N_7-C_{18} from O_3 of $n_2(O_3)\rightarrow\sigma^*(N_7\text{-}C_{18})$, N_2-C_{36} from O_4 of $n_2(O_4)\rightarrow\sigma^*(N_2\text{-}C_{36})$, N_2-C_{54} from O_5 of $n_2(O_5)\rightarrow\sigma^*(N_2\text{-}C_{54})$, N_7-C_{36} from N_6 of $n_1(N_6)\rightarrow\sigma^*(N_7\text{-}C_{36})$, N_6-C_{36} from N_7 of $n_1(N_7)\rightarrow\sigma^*(N_6\text{-}C_{36})$ with stabilization energies, 23.55, 52.13, 30.55, 30.40, 30.15, 16.28, 55.95 kJ/mol and electron densities, 0.36515, 0.24624, 0.09866, 0.09470, 0.09284, 0.05983, 0.36515e.

The natural hybrid orbitals with low occupation numbers and higher energies are: $n_2(S_1)$, $n_2(O_3)$, $n_2(O_4)$, $n_2(O_5)$ with energies, -0.25353, -0.24512, -0.26711, -0.26772 a.u and considerable p-characters, 99.99, 99.99, 100, 100% and low occupation numbers, 1.83619, 1.85326, 1.85149, 1.85466 while the orbitals with lower energies, high occupation numbers are: $n_1(S_1)$, $n_1(O_3)$, $n_1(O_4)$, $n_1(O_5)$ with energies, -0.63465, -0.6213, -0.68917, -0.69076a.u and p-character, 32.55, 41.85, 42.99, 42.76% and high occupation numbers, 1.98057, 1.97615, 1.97635, 1.97690. Thus, a very close to pure p-type lone pair orbital participates in the electron donation to the $n_1(S_1)\rightarrow\pi^*(N_6\text{-}C_{36})$, $n_1(N_2)\rightarrow\pi^*(O_5\text{-}C_{54})$, $n_2(O_3)\rightarrow\sigma^*(N_7\text{-}C_{18})$, $n_2(O_4)\rightarrow\sigma^*(N_2\text{-}C_{36})$, $n_2(O_5)\rightarrow\sigma^*(N_2\text{-}C_{54})$, $n_1(N_6)\rightarrow\sigma^*(N_7\text{-}C_{36})$ and $n_1(N_7)\rightarrow\sigma^*(N_6\text{-}C_{36})$ interactions in the compound.

4.7 Nonlinear Optical properties

In this work we are also reporting the results on the values of dipole moment, mean polarizability and first order hyperpolarizability. Dipole moment indicates the extent of charge separation within the molecule and can serve as an indicator of molecule's sensitivity to take part in reactions based on electrostatics. The higher the dipole moment is, the easier will molecule take part in electrostatic interactions with other structures. In this study we have obtained the value of 2.023 Debye for dipole moment of title molecule, which is relatively high value indicating possibly important electrostatic interaction with other molecules. Indirect measure of the extent of distortion in the electron density is represented by the polarizability. This quantity actually gives information on the response of molecular system under the influence of an external static electric field. It is also important to note that this parameter depends on the nature of bonding and geometrical structure of molecules. In this work we have calculated mean polarizability to have the value of 5.42×10^{-23} e.s.u. This value is higher than in the case of other dihydroquinazoline derivate that we have investigated in one of our previous works [71]. Analysis of organic molecules having conjugated π-electron systems and large hyperpolarizability using infrared and Raman spectroscopy has evolved as a subject of research [72]. The potential application of the title compound in the field of nonlinear optics demands the investigation of its structural and bonding features contributing to the hyperpolarizability enhancement, by analyzing the vibrational modes using the IR and Raman spectrum. The phenyl ring stretching bands at 1578, 1547, 1469, 1332, 1166, 1048 cm^{-1} observed in IR spectrum have their counterparts in the Raman spectrum at 1582, 1551, 1467, 1335, 1160, 1050 cm^{-1},

respectively and their intensities in IR and Raman spectra are comparable. The C-N bond lengths in the calculated molecular structure (C_{40}-N_2 = 1.4596, C_{43}-N_2 = 1.4069, C_{54}-N_2 = 1.4042, C_8-N_6 = 1.3824, C_{18}-N_7 = 1.4181, C_{36}-N_7 = 1.3835 Å) are intermediate between those of a C-N single bond (1.48 Å) and a C=N double bond (1.28 Å) and therefore, the calculated data suggest an extended π-electron delocalization of the molecular system which is responsible for the nonlinearity of the title compound [57]. The first order hyperpolarizability of the title compound is calculated and is found to be 3.07×10^{-30} esu and comparable with that of similar derivatives [55, 58] and 23.62 times that of the standard NLO material urea (0.13×10^{-30}esu) [73]. The average second hyperpolarizability is $\langle\gamma\rangle = (\gamma_{xxxx} + \gamma_{yyyy} + \gamma_{zzzz} + 2\gamma_{xxyy} + 2\gamma_{xxzz} + 2\gamma_{yyzz})/5$ [74]. The theoretical second order hyperpolarizability was calculated using the Gaussian09 software and is equal to -13.25×10^{-37} e.s.u and the reported value of a similar derivative is -56.01×10^{-37} e.s.u [75].

4.8 NMR spectra

The absolute isotropic chemical shielding (Table S3-supporting information) was calculated by B3LYP/GIAO model [76]. The experimental values are: ^{1}H NMR ($CDCl_3$): 8.10 (d, 1H, J = 7.5 Hz), 7.71 (dd, 2H, *J* = 3.0 Hz), 7.62–7.56 (m, 4H), 7.30 (t, 1H, *J* = 7.0 Hz), 7.21–7.21 (s, 4H), 7.15 (d, 1H, *J* = 3.5 Hz), 4.17 (t, 2H, *J* = 8.0 Hz), 4.10 (t, 2H, *J* = 6.5 Hz), 3.54 (t, 2H, *J* = 6.5 Hz), 2.94 (t, 2H, *J* = 8.0 Hz). ^{13}C NMR ($CDCl_3$): 30.0, 34.0, 37.0, 46.1, 119.4, 123.3, 125.8, 126.3, 126.7, 126.8, 128.6, 128.9, 131.9, 134.0, 134.3, 137.9, 147.3, 154.8, 161.5, 168.1. The experimental NMR spectra are given in Figs. S4 and S5 (supporting material). The protons of the phenyl rings resonate in the range 7.15-8.10 ppm experimentally and 7.6934-8.7619 ppm theoretically. The chemical shifts of the hydrogen atoms of the CH_2 group are observed in the range 2.94-4.17 ppm experimentally and 3.2758-5.0035 ppm theoretically. The ^{13}C NMR spectrum of the compound is also in agreement with number of carbon atoms present in the compound. The range of ^{13}C NMR chemical shifts of aromatic organic molecule is usually greater than 100 ppm [77, 78]. The studied molecule has eighteen carbon atoms and the chemical shifts values of aromatic carbon atoms are in the range 119.4-137.9 ppm experimentally and 121.5285-146.9905 ppm theoretically. The chemical shifts of C43, C54, C18 and C36 were observed in the range 147.3-168.1 ppm and the corresponding calculated values are in the range 158.8455-166.7041 ppm. The chemical shifts of the CH_2 carbon atoms were observed in the range 30.02-46.1 ppm while the calculated values are in the range 41.671-55.2868 ppm. Same as

in the case of IR and Raman spectroscopy, there is a good agreement between experimental and theoretical chemical shift of both ^{13}C and ^{1}H for the title compound, confirming the fact that the chosen level of theory is appropriate.

4.9 Reactive and degradation properties based on autoxidation and hydrolysis

Forced degradation studies are usual procedures for the investigation of stability of molecules with biological activity in the aquatic mediums, however such activities can be time consuming and complex. To overcome challenges related to experimental setup of forced degradation studies DFT calculations and MD simulations can be utilized for the assessment of degradation and stability properties [79-82]. In this regard it is important to mention the autoxidation mechanism, which can be initially assessed by DFT calculations of BDE for the hydrogen abstraction. Namely, during the process of autoxidation hydrogen atoms of drug candidate can be abstracted only at certain places where BDE values lie in the adequate interval. According to the study of Wright et al. [83] this interval is between 75 and 85 kcal/mol. This interval is in agreement with the values reported by to Gryn'ova et al. [84], who additionally state that thermodynamic favorability of C-H bond dissociation is questionable for the BDE values in the range between 85 and 90 kcal/mol.

Beside BDE values for hydrogen abstraction in this work we have also calculated BDE values for the rest of the single acyclic bonds. BDEs have been presented in the Fig. S6 (supporting information), where red color corresponds to the BDE values for hydrogen abstraction, while blue color corresponds to the BDE values for the rest of the single acyclic bonds. Results concerning the BDE values presented in Fig. S6 indicate that title molecule is highly stable towards the autoxidation mechanism since the lowest BDE value for hydrogen abstraction is significantly higher than the upper border limit of 90 kcal/mol. Concerning the BDE values for the rest of the single acyclic bonds the lowest one has been calculated in the case of bond denoted with number 15 with the corresponding value of 85 kcal/mol. Although the whole molecule is significantly stable, degradation process could start with the breaking of bond number 15. Although great stability has been confirmed by calculations of BDE for hydrogen abstraction we have also investigated the stability of title molecule in water. This is done by MD simulations and calculations of RDFs. RDF, g(*r*), determines the probability of finding a particle in the distance *r* from another particle [85] and Fig. S7 (supporting information) contains RDFs of title molecule's atoms with significant interactions with water molecules. Results presented in

Fig. S7 confirm high stability of title molecule. Namely, there are only five atoms with relatively significant interactions with water molecules, including atoms N2, O3, C18, C28 and C54. Of all mentioned atoms only oxygen atom O3 has peak distance located at below 3 Å (concretely at around 2.5 Å). Carbon atoms have peak distances located at around 3.5 Å. While peak distance of nitrogen atom N2 is located at around 4.7 Å. Weak possibilities for hydrolysis of investigated molecule are confirmed by absence of significant interactions between water molecules and hydrogen atoms of title molecule.

4.10 Molecular docking

Quinazolinones are a large class of active chemical compounds possessing a wide variety of biological activities such as anti HIV, anticancer [86], antifungal, antibacterial, anti-mutagenic, anticonvulsant etc. [87]. High resolution crystal structure of breast cancer type 2 complex was downloaded from the protein data bank website (PDB ID: 3EU7). All molecular docking calculations were performed on Auto Dock-Vina software [88] and as reported previously [89, 90]. Amongst the docked conformations, one which bonded well at the active site was analyzed for detailed interactions in Discover Studio Visualizer 4.0 software. The ligand binds at the active site of the substrate (Fig. 6) by weak non-covalent interactions. Amino acids Leu970, Pro924 and Met875 forms π-alkyl interaction with phenyl ring. Pro926 amino acid form π-alkyl interactions with pyrimidine ring. The docked ligand title compound forms a stable complex with breast cancer type 2 complex and gives a binding affinity (ΔG in kcal/mol) value of -7.9 (table 4). These preliminary results suggest that the compound might exhibit inhibitory activity against breast cancer type 2 complex.

5. Conclusion

A complete vibrational analysis of the title compound is performed by combining the experimental and theoretical information using density functional theory. The calculated HOMO and LUMO energies show that charge transfer occurs within the molecule. The location of HOMO indicates that the part of the molecule containing fused benzene and five membered ring could act as an electron donor, while LUMO designates mainly sulfur atom as the molecule location that could accept electrons. The calculated molecular electrostatic potential verifies the solid state interactions and determines molecular positions of oxygen atoms as prone to electrophilic attacks, since the lowest MEP values have been obtained precisely in the case of these atoms. The nonlinear optical properties are also addressed theoretically and the predicted

NLO properties of the title compound are much greater than that of urea and hence the title compound and its derivatives are a good candidate as second order NLO material. Stability of the molecular arising from hyperconjugative interactions, charge delocalization and intramolecular interactions has been analyzed using NBO analysis. Beside results concerning MEP surfaces, DFT calculations of ALIE values point sulfur atom S1 and carbon atoms of terminal benzene ring as possibly prone to electrophilic attacks. Fukui functions further indicated that molecule location where six and five-member rings are fuzzed is characterized by increasing charge density after the addition of charge, indicating that this part of molecule acts as an electrophile with the addition of charge. On the other side Fukui f^- function shows that molecule part in the near vicinity of oxygen atom O4 and hydrogen atoms H42 and H38 loses electron density after the removal of charge, designating this part of the molecule as nucleophilic, in the case when charge is removed. Analysis of charge density between non-bonded atoms indicated that three intra-molecular non-covalent interactions occur in the case of title molecule, with the strongest one between atoms S2 and H39. BDE values for hydrogen abstraction emphasize great stability of title molecule in the open air and in the presence of oxygen. This great stability is also confirmed in the water surrounding by RDFs after MD simulations, which have shown that only five atoms have relatively significant interactions with water molecules, neither one being hydrogen. From the molecular docking study shows that the ligand binds at the active site of the substrate by weak non-covalent interactions and the amino acids Leu970, Pro924 and Met875 forms π-alkyl interaction with phenyl ring. Pro926 amino acid form π-alkyl interactions with pyrimidine ring.

Acknowledgments

The authors extend their appreciation to the Deanship of Scientific Research at King Saud University for funding the work through the research group project No. RG-1435-046. The authors would like to thank the University of Antwerp for access to the university's CalcUA supercomputer cluster. Part of this work has been performed thanks to the support received form Schrödinger Inc.

References

[1] M. Hour, L. Huang, S. Kuo, Y. Xia, K. Bastow, Y. Nakanishi, E. Hamel, K.S. Lee, 6-alkylamino- and 2,3-dihydro-3-methoxy-2-phenl-4-quinazolinones and related

compounds, their synthesis, cytotoxicity and inhibition of tubulin polymerization, J. Med. Chem. 43 (2000) 4479-4487.

[2] R.J. Abdel-Jalil, W. Volter, M. Saeed, A novel method for the synthesis of 4(3H)-quinazolinones, Tetrahedron Lett. 45 (2004) 3475-3476.

[3] S.E. Lopez, M.E. Rosales, N. Urdaneta, M.V. Godoy, J.E. Charris, The synthesis of substituted 2-aryl 4(3H)-quinazolinones using NaHSO3/DMAc, steric effect upon the cycylization dehydrogenation step, J. Chem. Res. 6 (2000) 258-259.

[4] M.P. Hay, W.R. Wilson, J.W. Moselen, B.D. Palmer, W.A. Denny, Hypoxia-selective antitumor agents, 8. Bis(nitroimidazolyl)alkanecarboxamides, a new class of hypoxia selective cytotoxins and hypoxic cell radio sensitizers, J. Med. Chem. 19 (1994) 381-391.

[5] J.W. Corbett, S.S. Ko, J.D. Rodgers, L.A. Gearhart, N.A. Manus, L.T. Bachheler, S. Diamond, S. Jeffey, G.L. Trainor, P.S. Anderson, K. Erickson-Vitanen, Inhibition of clinically relevant mutant variants of HIV-1 by quinazolinone non-nucleoside reverse transcriptase inhibitors, J. Med. Chem. 43 (2000) 2019-2030.

[6] J.F. Liu, J. Lee, A.M. Dalton, G. Bi, L. Yu, C.M. Baldino, E. McElory, M. Brown, Microwave assisted one pot synthesis of 2,3-disubstituted 3H-quinazolin-4-ones, Tetrahedron Lett. 46 (2005) 1241-1244.

[7] I.A. Al-Suwaidan, A.A.-M. Abdel-Aziz, T.Z. Shawer, R.R. Ayyad, A.M. Alanazi, A.M. El-Morsy, M.A. Mohamed, N.I. Abdel-Aziz, M.A.-A. El-Sayed, A.S. El-Azab, Synthesis, antitumor activity and molecular docking study of some novel 3-benzyl-4(3H)quinazolinone analogues, J. Enzym. Inhib. Med. Chem. 31 (2016) 78-89.

[8] I.A. Al-Suwaidan, A.M. Alanazi, A.A.-M. Abdel-Aziz, M.A. Mohamed, A.S. El-Azab, Design, synthesis and biological evaluation of 2-mercapto-3-phenethylquinazoline bearing anilide fragments as potential antitumor agents, molecular docking study, Bioorg. Med. Chem. Lett. 23 (2013) 3935-3941.

[9] A.M. Alanazi, I.A. Al-Suwaidan, A.A.-M. Abdel-Aziz, M.A. Mohamded, A.M. El-Morsy, A.S. El-Azab, Design, synthesis and biological evaluation of some novel substituted 2-merpacto-3-phenethyl quinazolines as antitumor agents, Med. Chem. Res. 22 (2013) 5566-5577.

[10] A.S. El-Azab, M.A. Al-Omar, A.A.-M. Abdel-Aziz, N.I. Abdel-Aziz, A.-A. El-Sayed, A.M. Aleisa, M.M. Sayed-Ahmed, S.G. Abdel-Hamide, Design, synthesis and biological

evaluation of novel quinazoline derivatives as potential antitumor agents, molecular docking study, Eur. J. Med. Chem. 45 (2010) 4188-4198.

[11] A.S. El-Azab, K.E. ElTahir, Synthesis and anticonvulsant evaluation of some new 2,3,8-trisubstituted-4(3H)-quinazoline derivatives, Bioorg. Med. Chem. Lett. 22 (2010) 327-333.

[12] A.S. El-Azab, K.E. ElTahir, Design and synthesis of novel 7-aminoquinazoline derivatives, antitumor and anticonvulsant activities, Bioorg. Med. Chem. Lett. 22 (2010) 1879-1885.

[13] A.M. Alanazi, A.A.-M. Abdel-Aziz, I.A. Al-Suwaidan, S.G. Abdel-Hamide, T.Z. Shawer, A.S. El-Azab, Design, synthesis and biological evaluation of some novel substituted quinazolines as antitumor agents, Eur. J. Med. Chem. 79 (2014) 446-454.

[14] M.A. Mohamed, R.R. Ayyad, T.Z. Shawer, A.A.-M. Abdel-Aziz, A.S. El-Azab, Synthesis and antitumor evaluation of trimethoxy anilides based on 4(3H)-quinazolinone scaffolds, Eur. J. Med. Chem. 112 (2016) 106-113.

[15] W.T. Jiaang, Y.S. Chen, T. Hsu, S.H. Wu, C.H. Chien, C.N. Chang, S.P. Chang, S.J. Lee, X. Chen, Novel isoindoline compounds for potent and selective inhibition of prolyl dipeptidase DPP8, Bioorg. Med. Chem. Lett. 15 (2005) 687-691.

[16] J.F.M. Da Silva, S.J. Garden, A.C. Pinto, The chemistry of Isatins, a review from 1975 to 1999, J. Braz. Chem. Soc. (2001) 273-324.

[17] C.B. Cui, H. Kakeya, H. Osada, Novel mammalian cell cycle inhibitors, spirotryprostatins A and B, produced by aspergillus fumigates, which inhibit mammalian cell cycle at G2/M phase, Tetrahedron 52 (1996) 12651-12666.

[18] C. Fisher, C. Meyers, E.M. Carreira, Efficient synthesis of (±)-horsfiline through the MgI2-catalyzed ring expansion reaction of a spiro[cyclopropane-1,3'-indole]-2'-one, Helv. Chim. Acta 83 (2000) 1175-1181.

[19] P.B. Alper, C. Meyers, A. Lerchner, D.R. Siegel, E.M. Carreira, Facile, novel methodology for the synthesis of spiro[pyrrolidin-3,4'-oxindoles], catalyzed ring expansion reactions of cyclopropanes by aldimines, Angew. Chem. Int. Ed. 38 (1999) 3186-3189.

[20] A.M. Alanazi, A.A.-M. Abdel-Aziz, T.Z. Shawer, R.R. Ayyad, A.M. Al-Obaid, M.H. Al-Agamy, A.R. Maarouf, A.S. El-Azab, Synthesis, antitumor and antimicrobial activity of

some new 6-methyl-3-phenyl-4(3H)-quinazolinone analogues, in silico studies, J. Enzyme. Inhib. Med. Chem. 30 (2015) 1-15.

[21] S. Armaković, S.J. Armaković, J.P. Šetrajčić, I.J. Šetrajčić, Active components of frequently used β-blockers from the aspect of computational study. J. Mol. Model. 18 (2012) 4491-4501.

[22] B. Abramović, S. Kler, D. Šojić, M. Laušević, T. Radović, D. Vione, Photocatalytic degradation of metoprolol tartrate in suspensions of two TiO 2-based photocatalysts with different surface area. Identification of intermediates and proposal of degradation pathways. J. Hazard. Mater. 198 (2011) 123-132.

[23] S.J. Armaković, S. Armaković, N.L. Finčur, F. Šibul, D. Vione, J.P. Šetrajčić, B. Abramović, Influence of electron acceptors on the kinetics of metoprolol photocatalytic degradation in TiO 2 suspension. A combined experimental and theoretical study. RSC Advances. 5 (2015) 54589-54604.

[24] M. Blessy, R.D. Patel, P.N. Prajapati, Y. Agrawal, Development of forced degradation and stability indicating studies of drugs-A review, J. Pharm. Anal. 4 (2014) 159-165.

[25] J. Molnar, J. Agbaba, B. Dalmacija, M. Klašnja, M. Watson, M. Kragulj, Effects of ozonation and catalytic ozonation on the removal of natural organic matter from groundwater. J. Environ. Eng. 138 (2011), 804-808.

[26] D.D. Četojević-Simin, S.J. Armaković, D.V. Šojić, B.F. Abramović, Toxicity assessment of metoprolol and its photodegradation mixtures obtained by using different type of TiO 2 catalysts in the mammalian cell lines. Sci. Total Environ. 463 (2013) 968-974.

[27] P. Lienard, J. Gavartin, G. Boccardi, M. Meunier, Predicting drug substances autoxidation. Pharm. Res. 32 (2015), 300-310.

[28] G.L. de Souza, L.M. de Oliveira, R.G. Vicari, A. Brown, A DFT investigation on the structural and antioxidant properties of new isolated interglycosidic O-(1→ 3) linkage flavonols, J. Mol. Modeling, 22 (2016) 1-9.

[29] Z. Sroka, B. Żbikowska, J. Hładyszowski, The antiradical activity of some selected flavones and flavonols. Experimental and quantum mechanical study, J. Mol. Model. 21 (2015) 1-11.

[30] H. Djeradi, A. Rahmouni, A. Cheriti, Antioxidant activity of flavonoids: a QSAR modeling using Fukui indices descriptors, J. Mol. Model. 20 (2014) 1-9.

[31] Gaussian 09, Revision D.01, M.J. Frisch, G.W. Trucks, H.B. Schlegel, G.E. Scuseria, M.A. Robb, J.R. Cheeseman, G. Scalmani, V. Barone, B. Mennucci, G.A. Petersson, H. Nakatsuji, M. Caricato, X. Li, H.P. Hratchian, A.F. Izmaylov, J. Bloino, G. Zheng, J.L. Sonnenberg, M. Hada, M. Ehara, K. Toyota, R. Fukuda, J. Hasegawa, M. Ishida, T. Nakajima, Y. Honda, O. Kitao, H. Nakai, T. Vreven, J.A. Montgomery, Jr., J.E. Peralta, F. Ogliaro, M. Bearpark, J.J. Heyd, E. Brothers, K.N. Kudin, V.N. Staroverov, T. Keith, R. Kobayashi, J. Normand, K. Raghavachari, A. Rendell, J.C. Burant, S.S. Iyengar, J. Tomasi, M. Cossi, N. Rega, J.M. Millam, M. Klene, J.E. Knox, J.B. Cross, V. Bakken, C. Adamo, J. Jaramillo, R. Gomperts, R.E. Stratmann, O. Yazyev, A.J. Austin, R. Cammi, C. Pomelli, J.W. Ochterski, R.L. Martin, K. Morokuma, V.G. Zakrzewski, G.A. Voth, P. Salvador, J.J. Dannenberg, S. Dapprich, A.D. Daniels, O. Farkas, J.B. Foresman, J.V. Ortiz, J. Cioslowski, D.J. Fox, Gaussian, Inc., Wallingford CT, 2010.

[32] A. Irfan, R. Jin, A.G. Al-Sehemi, A.M. Asiri, Quantum chemical study of the donor acceptor triphenylamine based sensitizers, Spectrochim. Acta 110 (2013) 60-66.

[33] A. Irfan, A.G. Al-Sehemi, M.S. Al-Assiri, The effect of donors acceptors on the charge transfer properties and tuning of emitting color for thiophene, pyrimidine and oligoacene based compounds, J. Fluorine Chem. 157 (2014) 52-57.

[34] J.B. Foresman, in: E. Frisch (Ed.), Exploring Chemistry with Electronic Structure Methods: A Guide to Using Gaussian, Gaussian Inc., Pittsburg, PA, 1996.

[35] R. Dennington, T. Keith, J. Millam, GaussView, Version 5, Semichem Inc., Shawnee Mission KS, 2009.

[36] J.M.L. Martin, C. Van Alsenoy, GAR2PED, A Program to Obtain a Potential Energy Distribution from A Gaussian Archive Record, University of Antwerp, Belgium, 2007.

[37] A.D. Bochevarov, E. Harder, T.F. Hughes, J.R. Greenwood, D.A. Braden, D.M. Philipp, D. Rinaldo, M.D. Halls, J. Zhang, R.A. Friesner, Jaguar: A high performance quantum chemistry software program with strengths in life and materials sciences, Int. J. Quantum Chem. 113 (2013) 2110-2142.

[38] D. Shivakumar, J. Williams, Y. Wu, W. Damm, J. Shelley, W. Sherman, Prediction of absolute solvation free energies using molecular dynamics free energy perturbation and the OPLS force field, J. Chem. Theor. Comput. 6 (2010) 1509-1519.

[39] Z. Guo, U. Mohanty, J. Noehre, T.K. Sawyer, W. Sherman, G. Krilov, Probing the α-Helical Structural Stability of Stapled p53 Peptides: Molecular Dynamics Simulations and Analysis. Chem. Biol. Drug. Des. 75 (2010) 348-359.

[40] K.J. Bowers, E. Chow, H. Xu, R.O. Dror, M.P. Eastwood, B.A. Gregersen, J.L. Klepeis, I. Kolossvary, M.A. Moraes, F.D. Sacerdoti, *Scalable algorithms for molecular dynamics simulations on commodity clusters*. in *SC 2006 Conference, Proceedings of the ACM/IEEE*. 2006. IEEE.

[41] *Schrödinger Release 2015-4: Desmond Molecular Dynamics System, version 4.4, D. E. Shaw Research, New York, NY, 2015. Maestro-Desmond Interoperability Tools, version 4.4, Schrödinger, New York, NY, 2015.* 2015.

[42] A.D. Becke, Density-functional thermochemistry. III. The role of exact exchange, J. Chem. Phys. 98 (1993) 5648-5652.

[43] J.L. Banks, H.S. Beard, Y. Cao, A.E. Cho, W. Damm, R. Farid, A.K. Felts, T.A. Halgren, D.T. Mainz, J.R. Maple, Integrated modeling program, applied chemical theory (IMPACT). J. Comput. Chem. 26 (2005) 1752-1780.

[44] H.J. Berendsen, J.P. Postma, W.F. van Gunsteren, J. Hermans, *Interaction models for water in relation to protein hydration*, in *Intermolecular forces*. 1981, Springer. p. 331-342.

[45] A. Otero-de-la-Roza, E.R. Johnson, J. Contreras-García, Revealing non-covalent interactions in solids: NCI plots revisited. Phys. Chem. Chem. Phys. 14 (2012) 12165-12172.

[46] E.R. Johnson, S. Keinan, P. Mori-Sanchez, J. Contreras-Garcia, A.J. Cohen, W. Yang, Revealing noncovalent interactions. J. Am. Chem. Soc. 132 (2010) 6498-6506.

[47] R.T. Ulahannan, C.Y. Panicker, H.T. Varghese, R. Musiol, J. Jampilek, C. Van Alsenoy, J.A. War, A.A. Al-Saadi, Vibrational spectroscopic and molecular docking study of (2E)-N-(4-chloro-2-oxo-1,2-dihydroquinolin-3-yl)-3-phenylprop-2-enamide, Spectrochim. Acta 151 (2015) 335-349.

[48] Y.S. Mary, K. Raju, I. Yildiz, O. Temiz-Arpaci, H.I.S. Nogueira, C.M. Granadeiro, C. Van Alsenoy, FT-IR, FT-Raman, SERS and computational studyof 5-ethylsulphonyl-2-(o-chlorobenzyl)benzoxazole, Spectrochim. Acta 96 (2012) 617-625.

[49] A. Raj, Y.S. Mary, C.Y. Panicker, H.T. Varghese, K. Raju, IR, Raman, SERS and computational study of 2-(benzylsulfanyl)-3,5-dinitrobenzoic acid, Spectrochim. Acta 113 (2013) 28-36.

[50] Y.S. Mary, P.J. Jojo, C. Van Alsenoy, M. Kaur, M.S. Siddegowda, H.S. Yathirajan, H.I.S. Nogueira, S.M.A. Cruz, Vibrational spectroscopic studies (FT-IR, FT-Raman, SERS) and quantum chemical calculations on cyclobenzaprinium salicylate, Spectrochim. Acta 120 (2014) 340-350.

[51] G. Socrates, Infrared Characteristic Group Frequencies, John Wiley and Sons, New York, 1981.

[52] N.P.G. Roeges, A guide to the complete interpretation of IR spectra of Organic Compounds, Wiley, New York 1994.

[53] N.B. Colthup, L.H. Daly, S.E. Wiberly, Introduction to IR and Raman spectroscopy, Academic Press, New York 1990.

[54] R.M. Silverstein, F.X. Webster, Spectrometric Identification of Organic Compounds, 6th ed., John Wiley Asia, 2003.

[55] C.Y. Panicker, H.T. Varghese, K.R. Ambujakshan, S. Mathew, S. Ganguli, A.K. Nanda, C. Van Alsenoy, FT-IR and FT-Raman spectra and ab initio calculations of 3-{[(2-hydroxyphenyl)methylene]amino}-2-phenylquinazolin-4(3H)-one, J. Raman Spectrosc. 40 (2009) 1262-1273.

[56] G. Varsanyi, Assignments of Vibrational Spectra of Seven Hundred Benzene Derivatives, Wiley, New York 1974.

[57] A. Chandran, H.T. Varghese, C.Y. Panicker, C. VanAlsenoy, G. Rajendran, FT-IR and computational study (E)-N-caarbamimidoyl-4-((2-formylbenzylidene)amino)benzene sulfonamide, J. Mol. Struct. 1001 (2011) 29-35.

[58] C.Y. Panicker, H.T. Varghese, K.R. Ambujakshan, S. Mathew, S. Ganguli, A.K. Nanda, V. Van Alsenoy, Y.S. Mary, Ab initio and density functional theory studies on vibrational spectra of 3-{[(4-methoxyphenyl)methylene]amino}-2-phenylquinazolin-4(3H)-one, Eur. J. Chem. 1 (2010) 37-43.

[59] C.Y. Panicker, H.T. Varghese, K.R. Ambujakshan, S. Mathew, S. Ganguli, A.K. Nanda, C. Van Alsenoy, Y.S. Mary, Vibrational spectra and computational study of 3-amino—2-phenyl quinazolin-4(3H)-one, J. Mol. Struct. 963 (2010) 137-144.

[60] P. Thul, V.P. Gupta, V.J. Ram, P. Tandon, Structural and spectroscopic studies on 2-pyranones, Spectrochim. Acta 75 (2010) 251-260.

[61] J.S. Murray, J.M. Seminario, P. Politzer, P. Sjoberg, Average local ionization energies computed on the surfaces of some strained molecules. Int. J. Quantum Chem. 38 (1990) 645-653.

[62] P. Politzer, F. Abu-Awwad, J.S. Murray, Comparison of density functional and Hartree–Fock average local ionization energies on molecular surfaces. Int. J. Quantum Chem. 69 (1998) 607-613.

[63] A. Michalak, F. De Proft, P. Geerlings, R. Nalewajski, Fukui functions from the relaxed Kohn-Sham orbitals. J. Phys. Chem. 103A (1999) 762-771.

[64] R.G. Parr, W. Yang, Functional Theory of Atoms and Molecules, Oxford University Press, New York, 1989.

[65] P.W. Ayers, R.G. Parr, Variational principles for describing chemical reactions, the Fukui function and chemical hardness revisited, J. Am. Chem. Soc. 122 (2000) 2010-2018.

[66] P.K. Chattaraj, B. Maiti, U. Sarkar, Philicity, a unified treatment of chemical reactivity and selectivity, J. Phys. Chem. A 107 (2003) 4973-4975.

[67] C. Morell, A. Grand, A. Toro-Labbe, New dual descriptor for chemical reactivity, J. Phys. Chem. A 109 (2005) 205-212.

[68] R.G. Parr, P.K. Chattaraj, Principle of maximum hardness, J. Am. Chem. Soc. 113 (1991) 1854-1855.

[69] R.G. Parr, L. Szentpaly, Electrophilicity index, S. Liu, J. Am. Chem. Soc. 121 (1999) 1922-1924.

[70] E.D. Glendening, A.E. Reed, J.E. Carpenter, F.Weinhold, NBO Version 3.1, Gaussian Inc., Pittsburgh, PA, 2003.

[71] A.S. El-Azab, Y.S. Mary, C.Y. Panicker, A.A.-M. Abdel-Aziz, I.A. Al-Suwaidan, C. Van Alsenoy, FT-IR, FT-Raman and molecular docking study of ethyl 4-(2-(4-oxo-3-phenethyl-3,4-dihydroquinazolin-2-ylthio)acetamido)benzoate, J. Mol. Struct. 1111 (2016) 9-18.

[72] Y.S. Mary, C.Y. Panicker, H.T. Varghese, K. Raju, T.E. Bolelli, I. Yildiz, C.M. Granadeiro, H.I.S. Nogueira, Vibrational spectroscopic studies and computational study of 4-fluoro-N-(2'-hydroxy-4'-nitrophenyl)phenylacetamide, J. Mol. Struct. 994 (2011) 223-231.

[73] C. Adant, M. Dupuis, J.L. Bredas, Ab initio study of the nonlinear optical properties of urea, electron correlation and dispersion effects, Int. J. Quantum Chem. 56 (2004) 497-507.

[74] C. Hatting, O. Christiansen, P. Jorgensen, Frequency dependent second hyperpolarizabilities using coupled cluster cubic response theory, Chem. Phys. Lett. 282 (1998) 139-146.

[75] A.S. El-Azab, Y.S. Mary, C.Y. Panicker, A.A.-M. Abdel-Aziz, M.A. El-Sherbeny, C. Van Alsenoy, DFT and experimental (FT-IR and FT-Raman) investigation of vibrational spectroscopy and molecular docking studies of 2-(4-oxo-3-phenethyl-3,4-dihydroquinazolin-2-ylthio)-N-(3,4,5-trimethoxyphenyl)acetamide, J. Mol. Struct. 1113 (2016) 133-145.

[76] K. Wolinski, J.F. Hinton, P. Pulay, Efficient implementation of the gauge independent atomic orbital method for NMR chemical shift calculations, J. Am. Chem. Soc. 112 (1990) 8251-8260.

[77] A.R. Choudhury, T.N.G. Row, 5-fluorosalicylic acid, Acta Cryst. 60 (2004) o1595-o1597.

[78] Z. Liu, Y. Qu, M. Tan, H. Zhu, 5-bromosalicylic acid, Acta Cryst. E60 (2004) o1310-o1311.

[79] X.Ren, Y.Sun, X.Fu, L.Zhu, Z.Cui, DFT comparison of the OH-initiated degradation mechanisms for five chlorophenoxy herbicides. J. Mol. Model. 19 (2013) 2249-2263.

[80] L.-l .Ai, J.-y. Liu, Mechanism of OH-initiated atmospheric oxidation of E/Z-CF3CF= CFCF3: a quantum mechanical study. J. mol. Model. 20 (2014) 1-10.

[81] W. Sang-aroon, V. Amornkitbamrung, V. Ruangpornvisuti, A density functional theory study on peptide bond cleavage at aspartic residues: direct vs cyclic intermediate hydrolysis. J. Mol. Model. 19 (2013) 5501-5513.

[82] J. Kieffer, É. Brémond, P. Lienard, G. Boccardi, In silico assessment of drug substances chemical stability. J. Mol. Struct. THEOCHEM. 954 (2010) 75-79.

[83] J.S. Wright, H. Shadnia, L.L. Chepelev, Stability of carbon-centered radicals: Effect of functional groups on the energetics of addition of molecular oxygen. J. Comput. Chem. 30 (2009) 1016-1026.

[84] G. Gryn'ova, J.L. Hodgson, M.L. Coote, Revising the mechanism of polymer autooxidation. Org. Biomol. Chem. 9 (2011) 480-490.

[85] R.V. Vaz, J.R. Gomes, C.M. Silva, Molecular dynamics simulation of diffusion coefficients and structural properties of ketones in supercritical CO 2 at infinite dilution. J. Supercritic. Fluids 107 (2016) 630-638.

[86] D.K. Dodiya, S.J. Vaghasia, A.R. Trivedi, H.K. Ram, V.H. Shah, Synthesis, characterization and biological screening of some novel tetrahydroquinazoline derivatives, Indian J. Chem. 49 (2010) 802-806.

[87] R. Rajput, A. P. Mishra, A review on biological activity of quinazolinones, Int. J. Pharm. Pharm. Sci. 4 (2012) 66-70.

[88] O. Trott, A.J. Olson, AutoDock Vina, improving the speed and accuracy of docking with a new scoring function, efficient optimization and multithreading, J. Comp. Chem. 31 (2010) 455-461.

[89] V.V. Menon, E. Fazal, Y.S. Mary, C.Y. Panicker, S.Armakovic, S.J.Armakovic, S.Nagarajan, C. Van Alsenoy, FT-IR, FT-Raman and NMR characterization of 2-isopropyl-5-methylcyclohexyl quinoline-2-carboxylate and investigation of its reactive and optoelectronic properties by molecular dynamics simulations and DFT calculations, J. Mol. Struct. 1127 (2017) 124-137.

[90] B. Kramer, M. Rarey, T. Lengauer, Evaluation of the FlexX incremental construction algorithm for protein ligand docking, PROTEINS: Struct. Funct. Genet. 37 (1999) 228-241.

Figure captions

Fig.1 FT-IR spectrum of 2-(2-(4-oxo-3-phenethyl-3,4-dihydroquinazolin-2-ylthio)ethyl)isoindoline-1,3-dione

Table 1. Calculated (scaled) wavenumbers, observed IR, Raman bands and assignments of 2-(2-(4-oxo-3-phenethyl-3,4-dihydroquinazolin-2-ylthio)ethyl)isoindoline-1,3-dione

B3LYP/6-311++G(d,p)(5D,7F)			IR	Raman	Assignments[a]
υ(cm^{-1})	IR_I	R_A	υ(cm^{-1})	υ(cm^{-1})	-
3078	10.39	259.72	3082	3080	υCHPhII(91)
3077	10.98	286.74	-	-	υCHPhIII(99)
3073	2.78	39.78	-	-	υCHPhIII(95)
3072	1.86	97.10	-	-	υCHPhII(99)
3065	19.32	361.52	-	-	υCHPhI(93)
3063	5.27	147.62	-	-	υCHPhIII(100)
3060	10.00	169.14	-	3060	υCHPhII(99)
3054	25.60	50.73	3055	-	υCHPhI(98)
3051	1.40	62.75	-	-	υCHPhIII(94)
3046	6.68	94.28	-	-	υCHPhI(99)
3045	5.42	77.25	-	3043	υCHPhII(97)
3035	1.15	73.55	-	-	υCHPhI(96)
3032	8.32	28.43	-	-	υCHPhI(95)
3029	0.31	10.06	3027	-	υCH_2(100)
3013	6.54	14.01	-	-	υCH_2(93)
3012	0.81	33.12	-	2998	υCH_2(95)
2971	8.55	35.48	2976	-	υCH_2(96)
2963	9.94	70.23	-	-	υCH_2(94)
2962	9.32	21.02	-	-	υCH_2(94)
2953	2.22	171.28	2955	2956	υCH_2(100)
2928	11.96	108.98	-	2925	υCH_2(97)
1752	81.78	141.38	1760	1761	υC=O(79)
1700	644.28	11.35	1708	1715	υC=O(81)
1663	461.67	45.21	1668	1667	υC=O(73)
1582	46.89	82.19	-	1582	υPhII(63), δCHPhII(12)
1582	8.04	21.34	-	1582	υPhIII(56), δCHPhIII(11)

1580	1.79	32.24	-	1582	υPhIII(47), υPhI(14)
1580	9.87	46.04	1578	1582	υPhI(55), υPhIII(14)
1560	1.46	9.88	-	-	υPhI(69), δCHPhI(18)
1550	206.88	32.18	1547	1551	υCN(29), υPhII(58)
1526	300.38	257.44	-	-	υCN(40), υPhII(56)
1467	18.32	1.72	1469	1467	δCHPhI(21), υPhI(62)
1444	127.68	39.32	1446	-	δCHPhII(14), υCN(13), υPhII(52)
1441	13.85	4.91	-	-	δCH_2(91)
1438	6.43	3.95	-	1438	υPhIII(52), δCHPhIII(12)
1435	0.55	6.50	-	-	υPhIII(55), δCHPhIII(20)
1432	1.47	3.29	-	-	δCHPhII(24), υPhII(55)
1426	12.53	12.54	1428	-	δCHPhI(17), δCH_2(16), υPhI(58)
1425	6.02	42.32	-	-	δCH_2(68)
1423	38.41	58.67	-	-	δCH_2(87)
1389	3.71	52.87	1391	1393	δCH_2(85)
1356	173.16	46.64	1355	-	δCH_2(48), υCN(14)
1352	70.33	33.74	-	1349	δCH_2(66)
1331	59.65	18.33	1332	1335	δCH_2(42), υPhIII(46)
1324	45.41	50.74	-	-	δCH_2(56), υCN(14)
1322	175.54	36.54	-	1323	δCH_2(23), υCN(45)
1310	2.08	12.58	-	-	δCHPhI(70), δCH_2(10)
1308	175.92	20.61	-	-	δCH_2(50), υCN(21)
1306	43.27	107.54	-	1307	υPhII(80)
1290	3.25	3.04	-	-	υPhI(77)
1271	22.92	13.18	1275	1274	δCH_2(60)
1267	19.57	21.78	-	-	δCH_2(54), δCHPhII(16)
1259	0.79	0.24	-	-	δCHPhIII(63), δPhIV(11)
1256	49.75	52.17	-	-	δCH_2(17), δCHPhII(66)
1236	8.57	15.59	1238	1236	δCH_2(83)

1226	30.78	6.28	-	-	δCH_2(76)
1215	12.65	73.53	-	-	δCH_2(24), υCN(47)
1208	26.17	2.48	-	1206	δCHPhII(32), υCN(50)
1176	0.15	50.56	-	1180	υCC(37), δPhI(14), υPhI(11)
1163	14.71	95.63	1166	1160	υPhIII(46), υCC(24)
1156	0.17	3.56	-	-	δCHPhI(79), υPhI(14)
1152	19.45	2.31	1152	-	δCHPhII(57), υCN(40),
1143	3.97	5.84	-	-	δCHPhIII(43),υCC(21), υPhIII(13)
1136	0.85	4.31	-	-	δCHPhI(76), υPhI(16)
1135	6.00	11.03	-	1135	δCHPhIII(77), υPhIII(11)
1127	47.56	7.67	-	-	δCHPhII(56), υCN(10)
1109	122.30	14.39	1111	1106	δCH_2(25), υCN(43)
1084	0.77	3.11	1087	-	δCHPhII(26), υPhII(63)
1071	46.37	3.14	-	-	δCH_2(44), υCN(36)
1061	10.03	0.90	-	-	υPhI(26), δCHPhI(55)
1055	23.95	4.41	1048	1050	υPhIII(45), δCHPhIII(48),
1009	7.61	17.77	-	1012	υPhI(12), δPhI(13), δCHPhI(52)
1007	8.19	38.47	1005	1002	υPhII(21), δCHPhII(61)
999	3.01	3.04	-	-	υCC(64)
994	17.08	32.84	-	-	δCH_2(46), υPhIII(21)
992	15.00	24.39	-	-	υCC(20), υPhIII(25), δCH_2(15)
990	11.53	43.08	988	-	υCC(62), δCH_2(14)
978	0.03	49.99	-	980	δPhI(23), υPhI(63)
973	0.01	0.03	-	-	γCHPhIII(87), τPhIII(10)
967	0.03	0.14	-	969	γCHPhII(87), τPhII(11)
963	11.56	0.97	963	-	υCN(14), γCHPhI(52), τPhI(10)
962	7.49	2.19	-	-	γCHPhI(61)

955	35.28	0.70	-	-	δCH_2(40), υCN(46)
951	2.03	0.14	-	-	γCHPhII(90)
947	0.02	0.02	-	-	γCHPhI(91)
945	1.01	0.07	-	-	γCHPhIII(89)
938	15.21	3.38	-	-	υCN(39), δC=O(14), υPhIII(19)
891	1.05	4.46	893	-	γCHPhI(77), τPhI(11)
872	0.00	0.00	-	-	γCHPhIII(90)
869	13.69	5.19	868	869	δPhII(32), δPhV(12), υCN(12)
861	2.08	0.03	-	-	γCHPhII(82)
841	12.47	7.53	843	-	δPhIII(24), δC=O(46), υCC(15)
825	1.05	0.49	-	-	γCHPhI(80)
824	8.26	2.54	822	823	δPhII(10), υCS(10), υPhII(10)
799	6.92	29.05	796	796	υCC(16), υPhI(14), δPhI(15)
776	5.22	0.64	-	775	γC=O(41), τPhV(19), τPhII(14), γCHPhII(11)
773	5.37	1.91	-	-	γCHPhIII(49), γC=O(23), τPhIV(10)
766	0.65	0.26	768	-	τPhIII(31), γC=O(46), τPhIV(19)
753	58.12	0.90	-	754	γCHPhII(58), τPhII(19), τPhV(13)
741	13.43	4.23	-	-	τPhI(21), δCH_2(24), γCHPhI(11)
730	25.06	1.09	-	-	τPhI(18), δCH_2(51), γCHPhI(17)
729	18.03	28.02	-	-	υCS(49), δCH_2(20)
713	6.80	0.61	715	712	δCH_2(58), δPhIII(10)

697	60.01	6.94	695	696	γC=O(44), τPhIV(16), γCHPhIII(31)
692	14.57	9.92	-	-	δPhII(11), γCHPhI(15)
688	3.10	9.37	-	-	δPhIII(26), υCS(21)
684	45.89	1.57	-	-	τPhI(51), γCHPhI(23)
679	9.68	4.29	-	-	τPhII(35), γC=O(40), τPhI(10)
672	0.83	0.32	-	-	δPhIII(31), δC=O(43), δCH_2(19)
655	0.04	0.07	-	654	τPhIII(73), γC=O(13)
633	1.71	1.60	631	-	υCS(45), τPhV(33)
617	8.09	3.13	-	620	δPhII(23), δC=O(39)
611	0.35	3.91	613	-	δPhI(84)
592	19.12	23.72	593	-	δPhIV(49), δPhIII(10), δCN(11)
583	0.80	3.71	-	585	δPhII(48), υCS(17)
579	3.19	2.48	-	-	δPhI(39), δPhV(18), δPhII(10)
524	5.69	10.10	526	-	δPhV(42), δPhII(10)
516	10.58	0.40	-	-	δPhIV(24), τPhII(19), δPhIII(10)
516	7.65	0.22	-	-	τPhII(43), δPhIV(13)
513	17.65	3.04	-	509	δPhIII(18), δCS(10), δPhIV(10), δPhV(10)
493	10.70	0.84	-	-	τPhI(41), γCC(25), δPhI(13)
455	3.50	1.74	462	460	δPhV(26), δPhI(11), δCC(11)
448	0.01	0.12	445	-	τPhIII(73), τPhIV(10)
429	1.93	1.47	430	431	τPhII(58), τPhV(16)
400	1.07	0.53	-	402	τPhIII(71), τPhIV(16)
398	0.09	0.08	-	-	τPhI(83)
385	3.81	1.68	-	-	δCN(45), δC=O(19),

					δCC(10)
363	12.47	7.45	-	365	δCS(46), δPhV(12)
349	4.26	5.59	-	348	δC=O(25), δCH_2(10), γCC(16)
337	3.07	2.22	-	337	γCN(18), δCH_2(20), δCC(12), τPhI(12)
326	12.53	1.01	-	-	δCC(11), δC=O(17)
319	14.78	0.80	-	-	δCC(33), δCH_2(10)
299	1.33	1.92	-	302	δCH_2(36), γCN(19), δCS(14)
282	1.75	1.54	-	-	τPhII(22), δCN(11)
279	1.47	1.18	-	-	τPhII(35), τPhV(22)
263	2.27	1.42	-	264	δCN(39), δC=O(18)
237	2.22	2.83	-	239	τPhI(39), δCH_2(10)
229	0.01	0.96	-	-	δPhIII(25), δCC(20), δCN(10)
192	2.43	1.31	-	-	δCH_2(26), τCS(41)
176	0.93	1.13	-	-	τPhIV(27), δCS(26)
167	2.55	0.80	-	169	τPhIV(39), δCS(10)
148	0.46	1.14	-	150	τPhV(52), τPhII(15)
132	0.01	1.11	-	-	τPhIV(58), τPhIII(30)
130	2.54	0.43	-	-	τPhIV(45), γCN(29)
114	5.59	1.01	-	108	τPhV(32), γCN(18), τPhIV(10)
87	0.55	2.37	-	-	τPhV(31), τCS(11), τPhII(10)
82	0.00	4.12	-	-	γCC(25), δCH_2(25), τPhV(22)
61	0.04	0.82	-	-	τCH_2(50), τCC(25)
56	0.64	1.54	-	-	τCS(36), τCH_2(24), τPhV(10)
46	1.24	6.43	-	-	γCN(40), τCS(28)
34	0.24	1.28	-	-	τCC(28), τPhV(13), γCN(18), τCH_2(14)

28	0.27	4.09	-	-	τCC(39), τPhV(14), τCH_2(23)
21	0.01	0.54	-	-	τCH_2(55), τCS(13)
17	0.01	1.12	-	-	τCH_2(54), τCS(21)
14	0.28	2.33	-	-	τCS(37), γCN(21), τCH_2(18)
12	0.10	0.96	-	-	τCH_2(40), τCS(12)

[a]The C_{25}-C_{26}-C_{28}-C_{30}-C_{32}-C_{34} (mono), C_8-C_9-C_{11}-C_{13}-C_{15}-C_{17} (ortho) and C_{44}-C_{45}-C_{47}-C_{49}-C_{51}-C_{53} (ortho) phenyl rings are designated as PhI, PhII and PhIII respectively. he PhV-quinazoline ring; PhIV-isoindoline ring; υ-streching; δ-in-plane deformation; γ-out-of-plane deformation; τ-torsion; potential energy distribution (%) is given in the brackets in the assignment column.

Table 2

Second-order perturbation theory analysis of Fock matrix in NBO basis corresponding to the intramolecular bonds of the title compound.

Donor(i)	Type	ED/e	Acceptor(j)	Type	ED/e	E(2)[a]	E(j)-E(i)[b]	F(i,j)[c]
S1-C37	σ	1.59300	N2-C40	σ*	0.03072	3.00	0.94	0.047
-	-	-	N7-C36	σ*	0.05983	3.25	1.03	0.052
N2-C40	σ	1.98323	S1-C37	σ*	0.01926	2.10	0.91	0.039
-	-	-	N2-C43	σ*	0.09470	1.19	1.16	0.034
-	-	-	N2-C54	σ*	0.09284	1.23	1.16	0.034
-	-	-	C43-C44	σ*	0.07294	1.37	1.17	0.036
-	-	-	C53-C54	σ*	0.07319	1.50	1.17	0.038
N2-C43	σ	1.98422	N2-C40	σ*	0.03072	1.26	1.14	0.034
-	-	-	O5-C54	σ*	0.01078	3.53	1.40	0.063
-	-	-	C44-C45	σ*	0.02177	2.55	1.38	0.053
N2-C54	σ	1.98427	N2-C40	σ*	0.03072	1.22	1.14	0.033
-	-	-	O4-C43	σ*	0.01069	3.56	1.40	0.063
-	-	-	C51-C53	σ*	0.02181	2.58	1.38	0.053
O3-C18	π	1.98351	N7-C36	σ*	0.05983	1.70	1.49	0.046
-	-	-	C8-C17	σ*	0.03865	1.03	1.63	0.037
-	-	-	C17-C18	σ*	0.05990	2.05	1.54	0.051
-	-	-	C8-C17	π*	0.43255	4.24	0.40	0.041
O4-C43	π	1.97271	C44-C53	π*	0.41384	3.89	0.41	0.040
N6-C36	σ	1.98660	N6-C8	σ*	0.02520	1.81	1.38	0.045
-	-	-	N7-C19	σ*	0.02981	2.16	1.22	0.046
-	-	-	N7-C36	σ*	0.05983	1.63	1.33	0.042
-	-	-	C8-C9	σ*	0.02423	2.44	1.46	0.053
N7-C18	σ	1.98078	S1-C36	σ*	0.06017	3.19	0.96	0.050
-	-	-	N7-C19	σ*	0.02981	1.10	1.11	0.031
-	-	-	N7-C36	σ*	0.05983	2.10	1.22	0.046
-	-	-	C15-C17	σ*	0.02098	1.87	1.36	0.045
N7-C36	σ	1.98728	O3-C18	σ*	0.00854	2.04	1.45	0.049
-	-	-	N6-C36	σ*	0.01628	1.56	1.44	0.042
-	-	-	N7-C18	σ*	0.09866	1.27	1.24	0.036

-	-	-	N7-C19	σ*	0.02981	1.66	1.16	0.039
C8-C9	σ	1.97550	N6-C8	σ*	0.02520	1.61	1.17	0.039
-	-	-	N6-C36	σ*	0.01628	2.60	1.28	0.052
-	-	-	C8-C17	σ*	0.03865	3.62	1.25	0.060
-	-	-	C9-C11	σ*	0.01344	2.29	1.29	0.049
-	-	-	C17-C18	σ*	0.05990	2.88	1.16	0.052
C8-C17	σ	1.97309	O3-C18	σ*	0.00854	2.76	1.29	0.054
-	-	-	N6-C8	σ*	0.02520	1.27	1.18	0.035
-	-	-	C8-C9	σ*	0.02423	3.39	1.26	0.058
-	-	-	C15-C17	σ*	0.02098	4.02	1.27	0.064
-	-	-	C17-C18	σ*	0.05990	1.72	1.17	0.040
C17-C18	σ	1.97522	O3-C18	σ*	0.00854	1.49	1.28	0.039
-	-	-	N7-C19	σ*	0.02981	3.07	1.00	0.049
-	-	-	C8-C9	σ*	0.02423	2.72	1.24	0.052
-	-	-	C8-C17	σ*	0.03865	2.42	1.24	0.049
-	-	-	C13-C15	σ*	0.01388	1.99	1.28	0.045
-	-	-	C15-C17	σ*	0.02098	2.26	1.25	0.048
C19-C22	σ	1.97258	C25-C34	π*	0.34750	2.47	0.64	0.039
C37-C40	σ	1.98621	N2-C43	σ*	0.09470	1.01	1.03	0.029
C43-C44	σ	1.97262	N2-C40	σ*	0.03072	4.07	1.01	0.057
-	-	-	O4-C43	σ*	0.01069	1.14	1.27	0.034
-	-	-	C44-C45	σ*	0.02177	2.28	1.25	0.048
-	-	-	C44-C53	σ*	0.02696	1.74	1.23	0.041
-	-	-	C45-C47	σ*	0.01378	1.72	1.22	0.041
-	-	-	C51-C53	σ*	0.02181	4.06	1.25	0.064
C53-C54	σ	1.97310	N2-C40	σ*	0.03072	3.96	1.01	0.056
-	-	-	O5-C54	σ*	0.01078	1.12	1.27	0.03
-	-	-	C44-C45	σ*	0.02177	4.07	1.25	0.064
-	-	-	C44-C53	σ*	0.02696	1.76	1.23	0.042
-	-	-	C49-C51	σ*	0.01377	1.71	1.22	0.041
-	-	-	C51-C53	σ*	0.02181	2.32	1.25	0.048
LPS1	σ	1.98057	N6-C36	σ*	0.01628	3.09	1.23	0.055
-	π	1.83619	N2-C40	σ*	0.03072	1.18	0.59	0.024

-	-	-	N6-C36	π*	0.36515	23.55	0.25	0.072
-	-	-	C37-C40	σ*	0.02858	1.77	0.71	0.033
LPN2	σ	1.62446	S1-C37	σ*	0.01926	1.23	0.42	0.022
-	-	-	O4-C43	π*	0.24449	51.37	0.27	0.109
-	-	-	O5-C54	π*	0.24624	52.13	0.27	0.109
-	-	-	C37-C40	σ*	0.02858	6.37	0.62	0.062
LPO3	σ	1.97615	N7-C18	σ*	0.09866	1.51	1.07	0.037
-	-	-	C17-C18	σ*	0.05990	2.79	1.15	0.051
-	π	1.85326	N7-C18	σ*	0.09866	30.55	0.64	0.127
-	-	-	C17-C18	σ*	0.05990	17.87	0.72	0.104
LPO4	σ	1.97635	N2-C43	σ*	0.09470	2.16	1.09	0.044
-	-	-	C43-C44	σ*	0.07294	2.86	1.10	0.051
-	π	1.85149	N2-C43	σ*	0.09470	30.40	0.67	0.129
-	-	-	C43-C44	σ*	0.07294	21.17	0.68	0.109
LPO5	σ	1.97690	N2-C54	σ*	0.09284	2.06	1.10	0.043
-	-	-	C53-C54	σ*	0.07319	2.95	1.11	0.052
-	π	1.85466	N2-C54	σ*	0.09284	30.15	0.67	0.129
-	-	-	C53-C54	σ*	0.07319	21.14	0.68	0.109
LPN6	σ	1.88674	S1-C36	σ*	0.06017	3.80	0.50	0.039
-	-	-	N7-C36	σ*	0.05983	16.28	0.77	0.101
-	-	-	C8-C9	σ*	0.02423	1.52	0.90	0.034
-	-	-	C8-C17	σ*	0.03865	9.00	0.90	0.082
LPN7	σ	1.59300	O3-C18	π*	0.32182	49.15	0.28	0.107
-	-	-	N6-C36	π*	0.36515	55.95	0.26	0.109
-	-	-	C19-C22	σ*	0.02349	5.91	0.63	0.061

[a]E(2) means energy of hyper-conjugative interactions (stabilization energy in kJ/mol)

[b]Energy difference (a.u) between donor and acceptor i and j NBO orbitals

[c]F(i,j) is the Fock matrix elements (a.u) between i and j NBO orbitals

Table 3

NBO results showing the formation of Lewis and non-Lewis orbitals.

Bond(A-B)	ED/e[a]	EDA%	EDB%	NBO	s%	p%
σS1-C37	1.97658	48.62	51.38	$0.6973(sp^{4.97})S+$	16.65	83.35
-	-0.60345	-	-	$0.7168(sp^{4.00})C$	19.99	80.01
σN2-C40	1.98323	63.72	36.28	$0.7983(sp^{1.89})N+$	34.55	65.45
-	-0.75510	-	-	$0.6023(sp^{3.63})C$	21.59	78.41
σN2-C43	1.98422	63.74	36.26	$0.7984(sp^{2.04})N+$	32.84	67.16
-	-0.80105	-	-	$0.6022(sp^{2.35})C$	32.84	67.16
σN2-C54	1.98427	63.65	36.35	$0.7978(sp^{2.07})N+$	332.56	67.44
-	-0.80223	-	-	$0.6029(sp^{2.34})C$	29.87	70.13
πO3-C18	1.98351	69.78	30.22	$0.8354(sp^{1.00})O+$	0.00	100.0
-	-0.36420	-	-	$0.5497(sp^{1.00})C$	0.00	100.0
πO4-C43	1.97271	67.93	32.07	$0.8242(sp^{1.00})O+$	0.00	100.0
-	-0.38931	-	-	$0.5663(sp^{1.00})C$	0.00	100.0
σN6-C36	1.98660	59.04	40.96	$0.7684(sp^{1.58})N+$	38.64	61.36
-	-0.90106	-	-	$0.6400(sp^{1.67})C$	37.48	62.52
σN7-C18	1.98078	64.51	35.49	$0.8032(sp^{2.02})N+$	33.09	66.91
-	-0.79031	-	-	$0.5958(sp^{2.48})C$	28.67	71.33
σN7-C36	1.98728	62.55	37.45	$0.7909(sp^{1.88})N+$	34.74	65.26
-	-0.84633	-	-	$0.6119(sp^{1.95})C$	33.88	66.12
σC8-C9	1.97550	51.34	48.66	$0.7165(sp^{1.80})C+$	35.71	64.29
-	-0.68483	-	-	$0.6976(sp^{1.95})C$	33.86	66.14
σC8-C17	1.97309	49.28	50.72	$0.7020(sp^{1.82})C+$	35.48	64.52
-	-0.69507	-	-	$0.7122(sp^{1.95})C$	33.84	66.16
σC17-C18	1.97522	51.60	48.40	$0.7183(sp^{2.26})C+$	30.68	69.32
-	-0.67659	-	-	$0.6957(sp^{1.59})C$	38.54	61.46
σC19-C22	1.97258	50.43	49.57	$0.7102(sp^{2.51})C+$	28.48	71.52
-	-0.59699	-	-	$0.7040(sp^{2.94})C$	25.40	74.60
σC37-C40	1.98621	50.63	49.37	$0.7115(sp^{2.45})C+$	28.98	71.02
-	-0.62755	-	-	$0.7026(sp^{2.62})C$	27.64	72.36
σC43-C44	1.97262	47.78	52.22	$0.6912(sp^{1.75})C+$	36.30	63.70
-	-0.66985	-	-	$0.7226(sp^{2.38})C$	29.54	70.46
σC53-C54	1.97310	52.19	47.81	$0.7224(sp^{2.38})C+$	29.56	70.44

-	-0.67080	-	-	0.6915($sp^{1.75}$)C	36.34	63.66
n1S1	1.98057	-	-	$sp^{0.48}$	67.45	32.55
-	-0.63465	-	-	-	-	-
n2S1	1.83619	-	-	$sp^{1.00}$	0.01	99.99
-	-0.25353	-	-	-	-	-
n1N2	1.62446	-	-	$sp^{1.00}$	0.01	99.99
-	-0.26777	-	-	-	-	-
n1O3	1.97615	-	-	$sp^{0.71}$	58.15	41.85
-	-0.6213	-	-	-	-	-
n2O3	1.85326	-	-	$sp^{99.99}$	0.01	99.99
-	-0.24512	-	-	-	-	-
n1O4	1.97635	-	-	$sp^{0.75}$	57.01	42.99
-	-0.68917	-	-	-	-	-
n2O4	1.85149	-	-	$sp^{1.00}$	0.00	100.0
-	-0.26711	-	-	-	-	-
n1O5	1.97690	-	-	$sp^{0.75}$	57.24	42.76
-	-0.69076	-	-	-	-	-
n2O5	1.85466	-	-	$sp^{1.00}$	0.00	100.0
-	-0.26772	-	-	-	-	-
n1N6	1.88674	-	-	$sp^{2.70}$	27.01	72.99
-	-0.33709	-	-	-	-	-
n1N7	1.59300	-	-	$sp^{99.99}$	0.01	99.99
-	-0.26584	-	-	-	-	-

[a] ED/e is expressed in a.u.

Table 4

The binding affinity values of different poses of the title compound predicted by AutodockVina.

Mode	Affinity (kcal/mol)	Distance from best mode (Å)	
-	-	RMSD l.b.	RMSD u.b.
1	-7.9	0.000	0.000
2	-7.9	2.496	4.010
3	-7.8	2.088	4.206
4	-7.7	3.098	6.980
5	-7.7	1.702	2.673
6	-7.4	3.151	6.876
7	-7.4	4.040	7.289
8	-7.4	2.197	5.842
9	-7.4	3.305	7.869

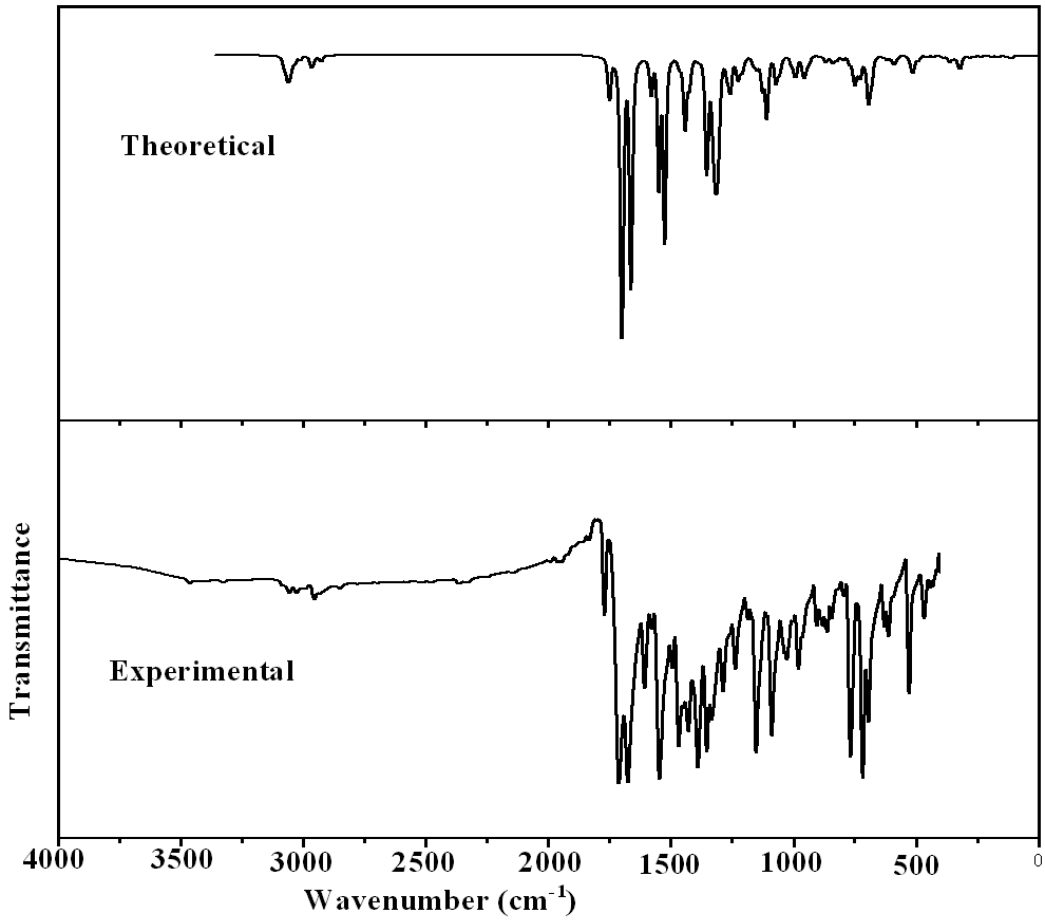

Fig.1 FT-IR spectrum of 2-(2-(4-oxo-3-phenethyl-3,4-dihydroquinazolin-2-ylthio) ethyl)isoindoline-1,3-dione

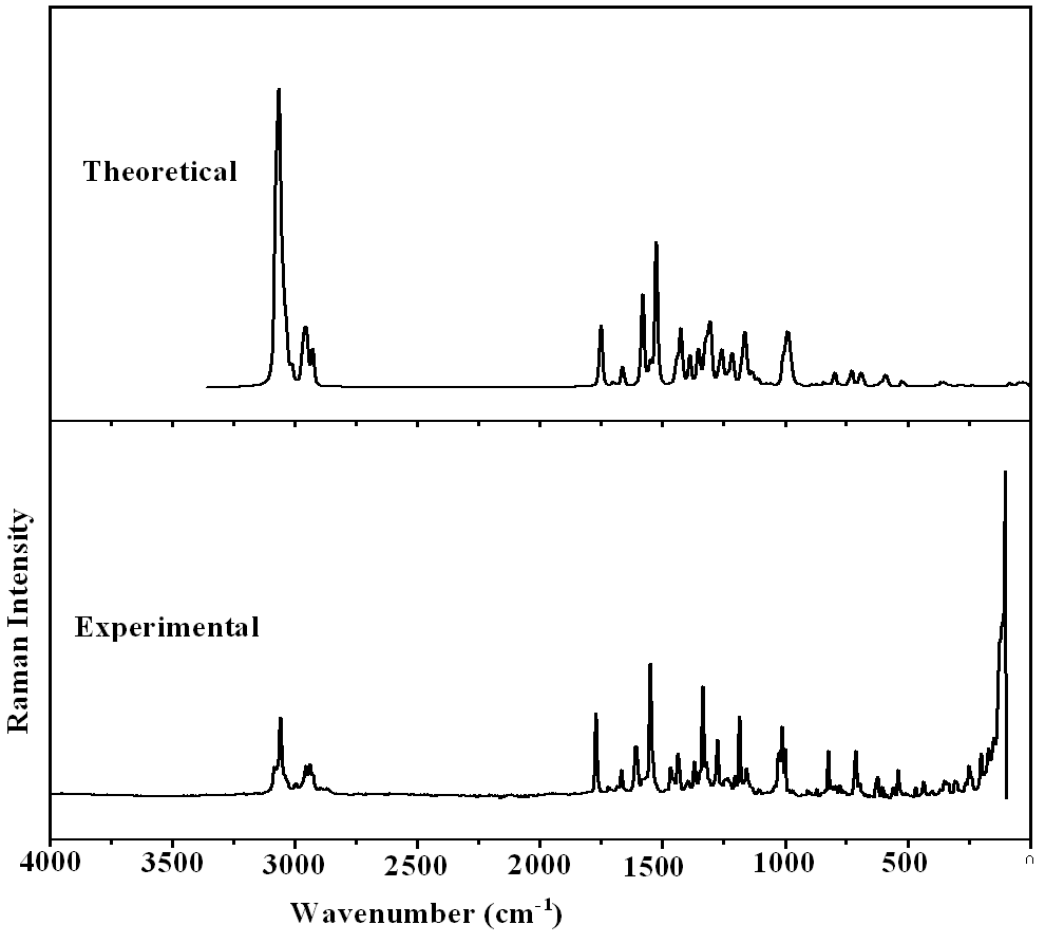

Fig.2 FT-Raman spectrum of 2-(2-(4-oxo-3-phenethyl-3,4-dihydroquinazolin-2-ylthio) ethyl)isoindoline-1,3-dione

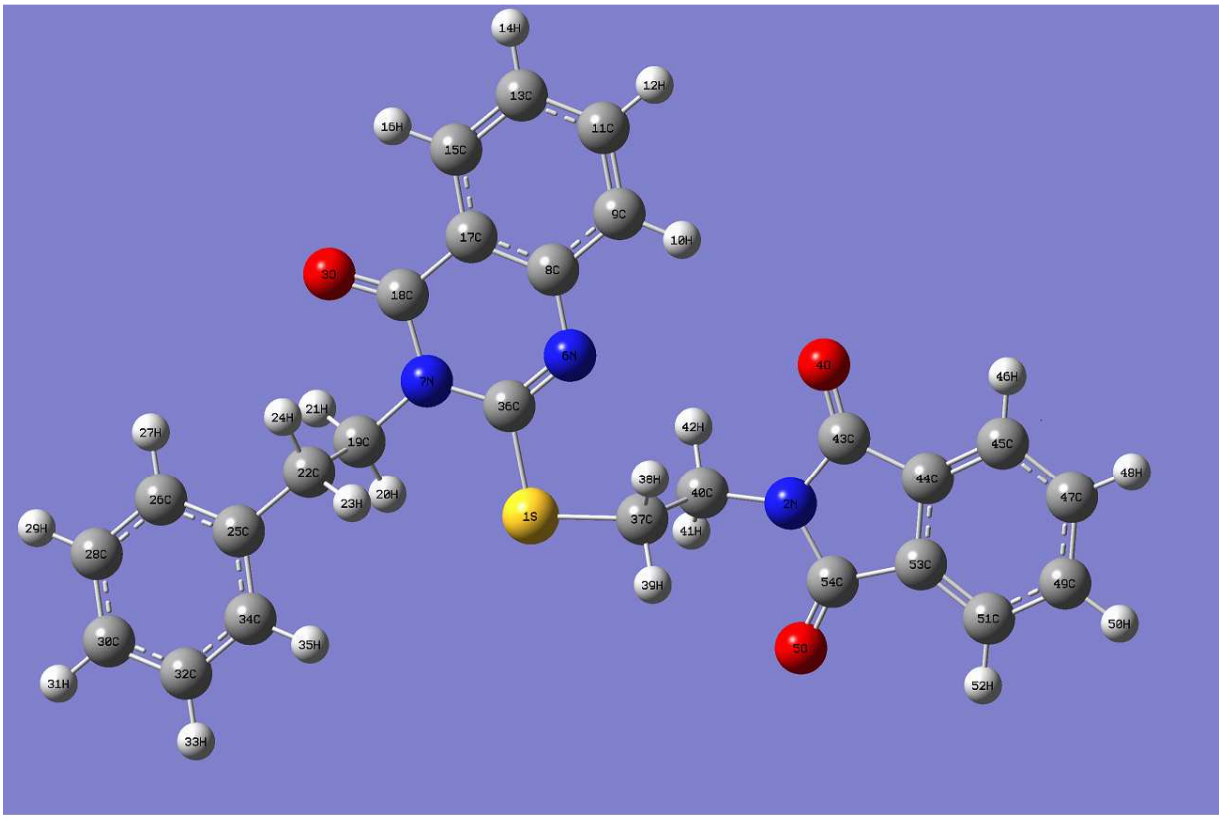

Fig.3 Optimized geometry of 2-(2-(4-oxo-3 -phenethyl-3,4-dihydroquinazolin-2-ylthio) ethyl)isoindoline-1,3-dione

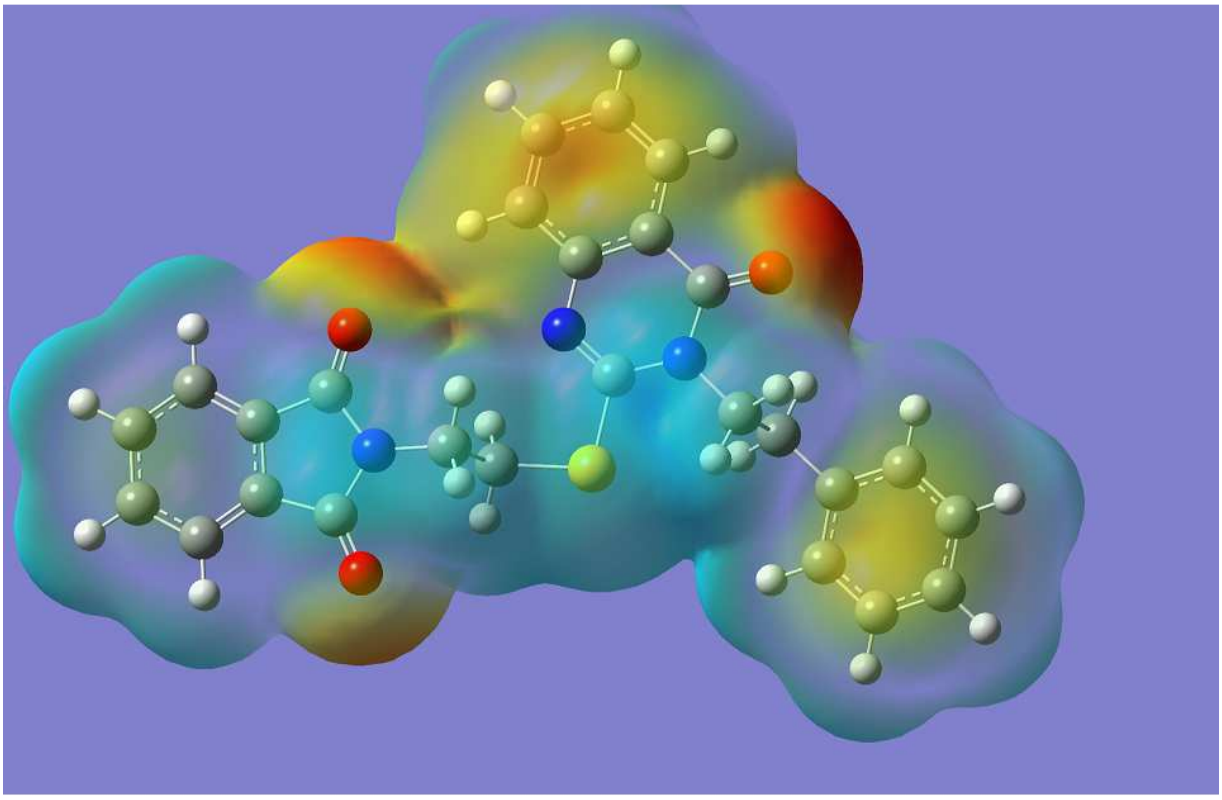

Fig.4 MEP plot of 2-(2-(4-oxo-3-phenethyl-3,4-dihydroquinazolin-2-ylthio)ethyl)isoindoline-1,3-dione

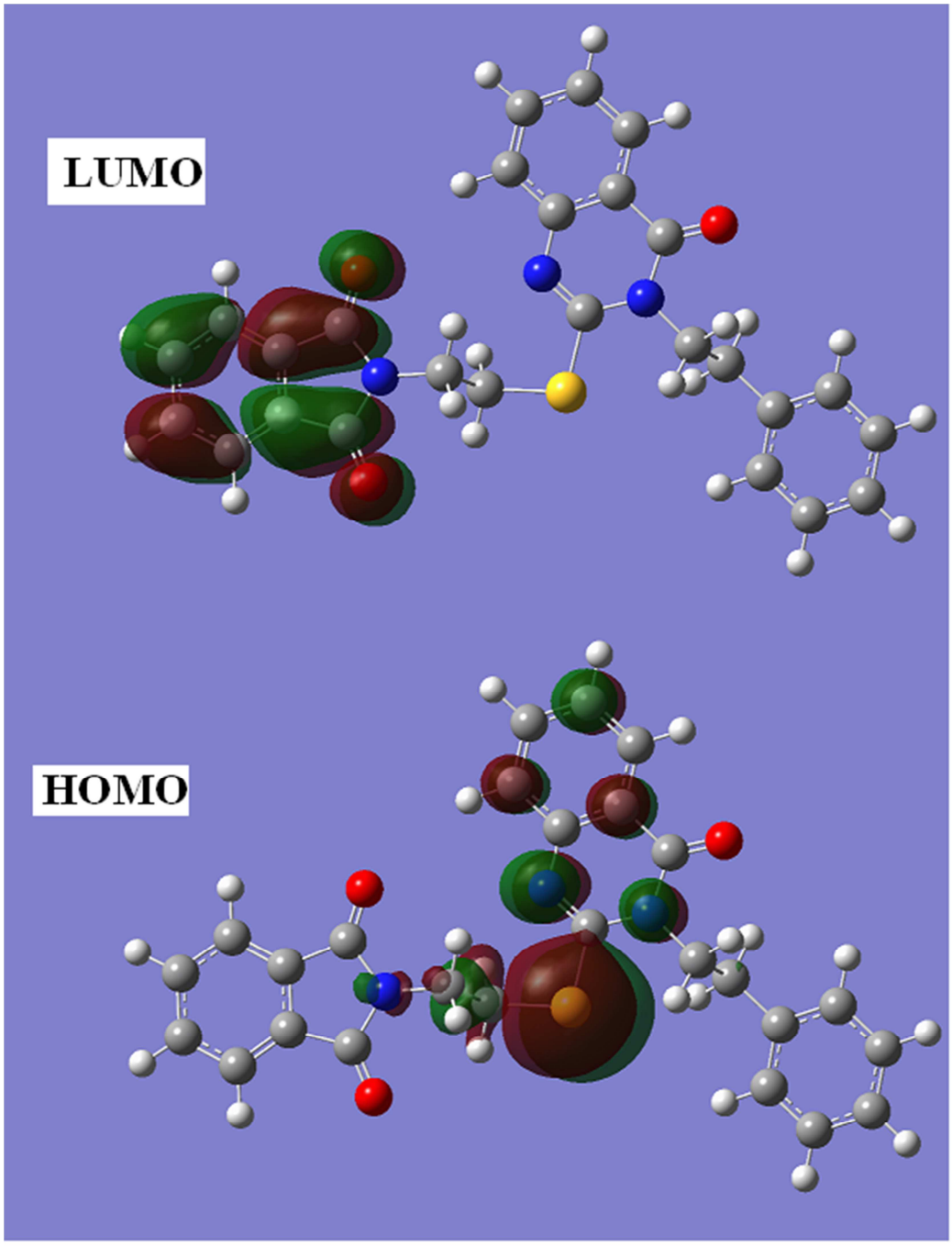

Fig.5 HOMO-LUMO plots of 2-(2-(4-oxo-3-phenethyl-3,4 -dihydroquinazolin-2-ylthio)ethyl) isoindoline-1,3-dione

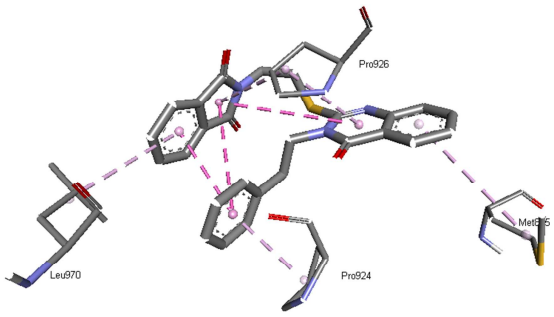

Fig.6a Schematic for the docked conformation of active site of title compound at breast cancer type 2 complex

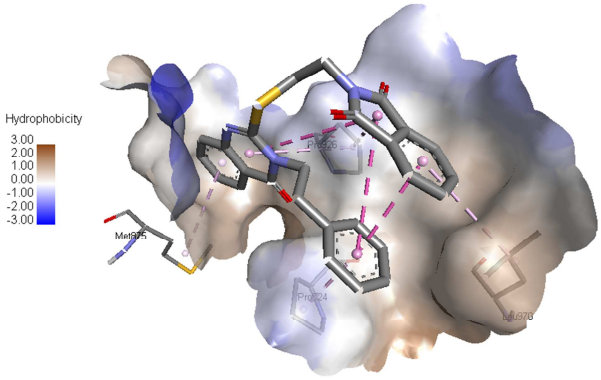

Fig.6b The docked protocol reproduced the co-crystallized conformation with π-alkyl (pink) and hydrophobic receptor surface shown.

Highlights

* IR, Raman, docking studies were reported
* Most reactive sites are predicted by using MEP plot
* BDEs are calculated to investigate autoxidation and degradation properties
* The compound exhibits inhibitory activity against breast cancer type 2 complex